NOTICE

The quality of this microform is heavily dependent upon the quality of the original thesis submitted for microfilming. Every effort has been made to ensure the highest quality of reproduction possible.

If pages are missing, contact the university which granted the degree.

Some pages may have indistinct print especially if the original pages were typed with a poor typewriter ribbon or if the university sent us an inferior photocopy.

Previously copyrighted materials (journal articles, published tests, etc.) are not filmed.

Reproduction in full or in part of this microform is governed by the Canadian Copyright Act, R.S.C. 1970, c. C-30

AVIS

La qualité de cette microforme dépend grandement de la qualité de la thèse soumise au microfilmage. Nous avons tout fait pour assurer une qualité supérieure de reproduction.

S'il manque des pages, veuillez communiquer avec l'université qui a conféré le grade.

La qualité d'impression de certaines pages peut laisser à désirer, surtout si les pages originales ont été dactylographiées à l'aide d'un ruban usé ou si l'université nous a fait parvenir une photocopie de qualité inférieure.

Les documents qui font déjà l'objet d'un droit d'auteur (articles de revue, tests publiés, etc.) ne sont pas microfilmés.

La reproduction, même partielle, de cette microforme est soumise à la Loi canadienne sur le droit d'auteur, SRC 1970, c. C-30

Canada

Cytochrome c Oxidase and Metalloderivatives of Cytochrome c

Monique Marie Laberge

A Thesis

in

The Department

of

Chemistry

Presented in Partial Fulfillment of the Requirements
for the Degree of Master of Science at
Concordia University
Montréal, Québec, Canada

August 1988

ISBN 0-315-44829-6

ABSTRACT

Cytochrome c Oxidase and Metalloderivatives of Cytochrome c

Monique Marie Laberge

The tin, zinc and europium derivatives of horse heart cytochrome c were prepared and characterized as follows: Zinc cytochrome c has absorption maxima at 422, 549 and 583 nm and fluorescence emission maxima at 590 and 640 nm (τ = 1.4 ns). Tin cytochrome c has absorption maxima at 410,535 and 574 nm. Its fluoresecnce emission maxima are at 580 and 636 nm. Two components are observed in the emission with respective lifetimes of 1.6 and 0.4 ns. Europium cytochrome c has a Soret maximum at 403 nm with visible maxima at 501, 534, 556 and 610 nm. Fluorescence emission maxima occur at 619 and 669 nm. At low ionic strength, the tin and zinc derivatives bind cytochrome c oxidase in the ratio of one Snc or Znc per $aCu_A a_3 Cu_B$. In the presence of cytochrome c oxidase, the triplet absorption decay of Znc (92 s^{-1}) is quenched. Two components are observed in the decay profile of the complex: a process with k = 668 s^{-1} and a slower one with k = 330 s^{-1}. Radiationless dipole-dipole transfer of triplet excitation energy to the oxidase is believed to be the predominant quenching mechanism. Calculations of intermolecular separation yield donor-acceptor distances of 13 and 15 A. This is consistent with the conclusion that the acceptors are two copper atoms of the oxidase.

ACKNOWLEDGEMENTS

The author wishes to express her sincere appreciation to all those who provided a helping hand in any part of the work on which this thesis is based. In particular, to Dr. J. A. Kornblatt, in whose laboratory the work was carried out and for his helpful suggestions and to the many kind faculty members, colleagues and support staff in the department without whose support this work would have been much more difficult: Dr. G. Denes, Dr.J. Capobianco, Dr. R. Rye, Dr. B. Hill, Dr.N. Serpone and T.C. Cheung. Also, special thanks to fellow graduate students for their interest, willingness to help and much more: P. Taslimi, A. Peters and D. Biro. Last but not least, I would like to acknowledge the advice and help of Mr. Christie and his coworkers and thank them for their patience and good spirits.

" cha'n eil eadar an t-amadan, agus an duine ghi ach tairgse m'baith a ghabhail, 'nnair a gheibhe'i ..."

TABLE OF CONTENTS

LIST OF FIGURES

LIST OF TABLES

LIST OF SYMBOLS AND ABBREVIATIONS

$aCu_A a_3 Cu_B$: cytochrome c oxidase

aa_3: cytochrome c oxidase, fully oxidized

$a^2 a_3^2$: cytochrome c oxidase, fully reduced form

c^{-Fe}: iron-free cytochrome c

porphyrin c: iron-free cytochrome c

c : native cytochrome c

Euc: Europium cytochrome c

Snc: Tin cytochrome c

Znc: Zinc cytochrome c

^{3}Znc: Triplet state of zinc cytochrome c

EDTA: Ethylenediaminetetraacetic acid

KPi: Potassium phosphate buffer

HIS: Histidine

MET: Methionine

TRP: Tryptophan

1.INTRODUCTION

Metalloporphyrins dominate the energy/electron transfer processes of many biological systems. In recent years, a consensus seems to have emerged in the haem protein field that most of these processes primarily depend on long range electron transfer covering distances of some 10 to 30 A [McLendon, 1988].

Several experimental approaches have been used to study these questions , most of them successful at confirming theoretical predictions. Consider for example the work of Miller which established the exponential dependence of electron transfer rates on distance [Miller, 1975], a prediction of Marcus theory [Marcus, 1956], and, among the most recent efforts, that of groups providing experimental evidence for the predicted dependence of rate on free energy [Conklin-Taylor,1988].

Of course, these attempts at correlating theory and observations would not have been possible without first obtaining answers as to how the carriers are physically organized so as to promote effective electron/energy flow. Central to the study of these questions are naturally occurring carriers such as haem proteins, among which cytochrome c has been the most exhaustively studied.

Haem proteins are characterized by the presence of one or more haem groups in their structure. The central feature of all haem proteins is the prosthetic group. For several, it

FIGURE 1.1

IRON(II)PROTOPORPHYRIN - All eight pyrrole carbons are completely substituted on the porphyrin ring. The nature of the substituents provides additional stabilizing interaction between the haem and the protein matrix in haemproteins. The metal is four-coordinate with a slightly distorted square-planar environment. Two pyrrole rings are tilted up and two are tilted down so that the nitrogens are out of plane. The iron-nitrogen bond length is 1.96 A. Addition of one axial ligand produces a five-coordinate square-pyramidal species while that of two ligands yields a six-coordinate distorted octahedral structure. [Hughes, 1984]

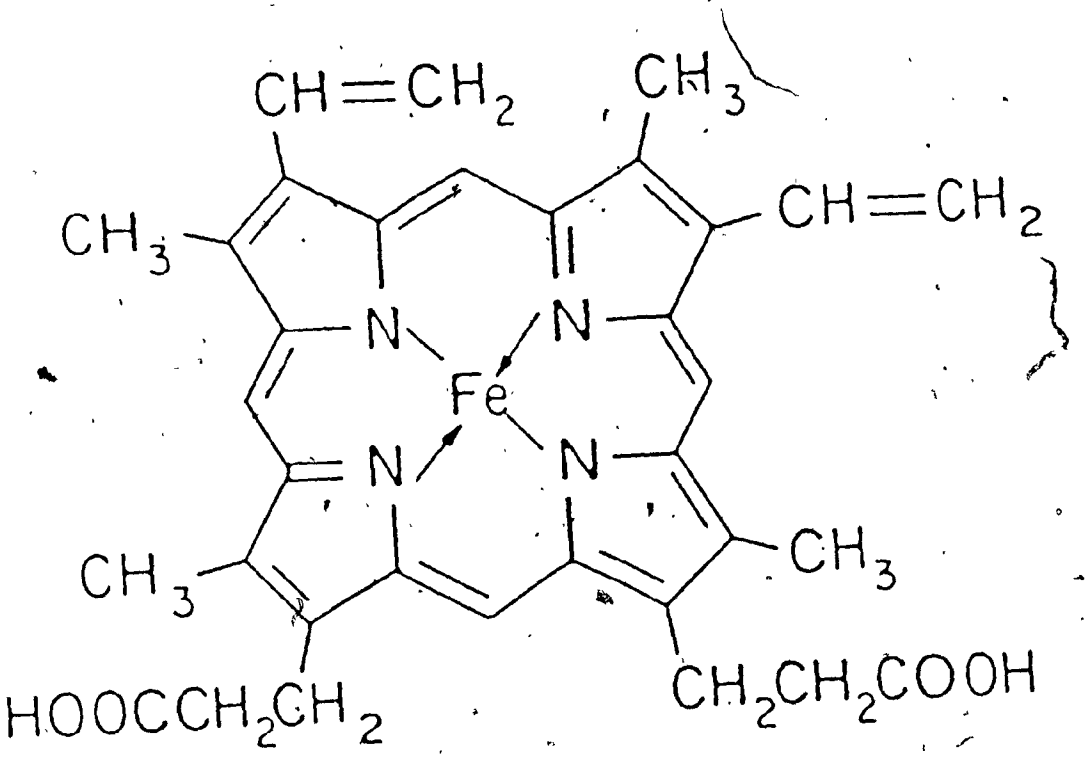
CH=CH2
CH3
CH3
CH=CH2
N
N
Fe
N
N
CH3
CH3
HOOCCH2CH2
CH2CH2COOH

consists of protohaem--iron(II)protoporphyrin IX (Fig 1.1). The porphyrin ring is a roughly planar ensemble of several dozen atoms with a central iron atom covalently bound to four nitrogens. Ring substituents include four methyls, two propionic acids and two vinyl side chains. In cytochrome c (Fig 1.2) the haem has a polypeptide chain attached and wrapped around it. Horse heart cytochrome c has a molecular weight of 12,400 and its polypeptide chain contains 104 amino acid residues. A nitrogen atom from a histidine residue (his-18) and a sulphur atom from a methionine residue (met-80) of this chain are coordinated to the 5th and 6th coordination sites of the iron. Its function is to shuttle electrons, which it accepts from a reductase and conveys to cytochrome c oxidase for the reduction of dioxygen to water. The polypeptide chain also accounts for the binding properties of cytochrome c to its partners by providing specificity and proper orientation of the haem edges, mediated by complementary charge interactions (Fig 1.3). [Salemme,1977;Koppenol,1982]. In earlier days, there used to be an even split in the haem protein field with respect to deciding whether the metal or the protein moiety was responsible for the efficiency of biological electron transfer and the specificity of the haem partners. People trained as inorganic chemists would sing the praise of the transition metal in the porphyrin hole, while biochemists would argue about the importance of a given amino acid residue. Fortunately for the problem under consideration, the

FIGURE 1.2

SCHEMATIC REPRESENTATION OF CYTOCHROME c - The haem is six-coordinate and covalently bound to the protein via thioether groups. X-ray results show that the axial ligands are his-18 and met-80 in both oxidation states. Cytochrome c accepts an electron from cytochrome c_1 and transfers it to cytochrome c oxidase. Heavy circles illustrate deeply buried residues and filled circles the haem contact residues. Many exposed residues are mobile while the haem contact residues seldom flip, with the exception of residues linked to reactivity such as phe-82. [Campbell,1985]

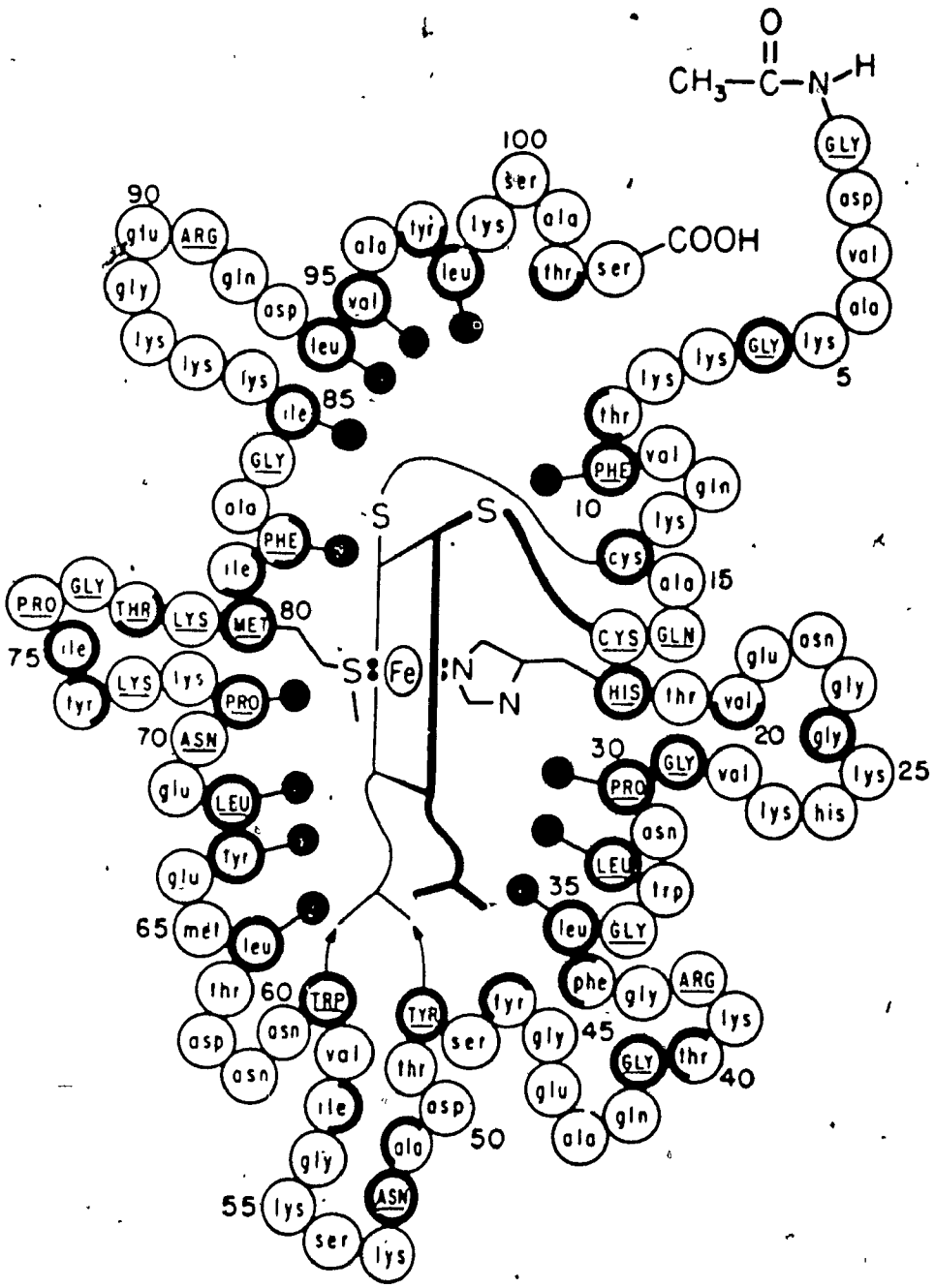
CH3—C—N—H
O
COOH
GLY
asp
val
ala
lys
GLY
lys
5
lys
thr
PHE
val
gln
10
lys
cys
ala
15
CYS
GLN
glu
asn
gly
gly
lys
25
HIS
thr
val
20
30
PRO
GLY
val
lys
his
asn
LEU
trp
35
leu
GLY
phe
gly
ARG
lys
GLY
thr
40
glu
gln
ala
45
tyr
ser
gly
TYR
thr
asp
50
ala
ASN
lys
ser
55
lys
gly
ile
val
asn
asp
thr
60
TRP
leu
met
65
tyr
glu
LEU
glu
ASN
70
PRO
lys
LYS
tyr
ile
75
PRO
GLY
THR
LYS
MET
80
S
Fe
N
N
S
S
ile
85
GLY
ala
PHE
ile
lys
lys
lys
gly
glu
ARG
gln
asp
leu
val
95
ala
tyr
lys
ala
ser
thr
leu
100
ser
90

FIGURE 1.3

SCHEMATIC REPRESENTATION OF THE DOMAINS ON CYTOCHROME c FOR THE INTERACTION WITH ITS PARTNERS - The rectangle represents the solvent-accessible haem edge. The number of circles around a given lysyl residue is proportional to the dipole strength. The numbers indicate the relative position of the residues in the chain. Cytochrome c must therefore be correctly oriented with complementary electrostatic fields and molecular dipoles. The rate of electron transfer is sensitive to changes in the cytochrome c dipole. [Koppenol,1982]

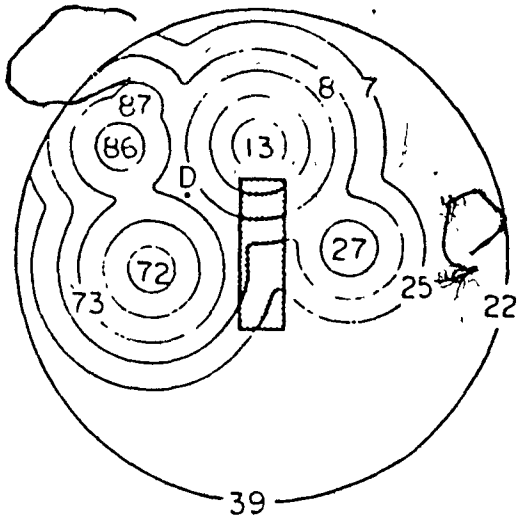

CYTOCHROME *c* REDUCTASE

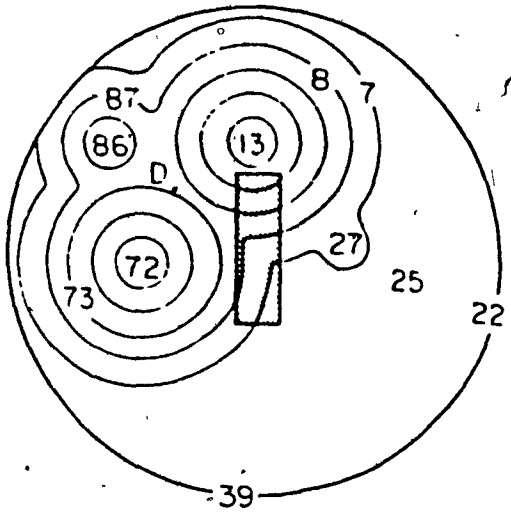

CYTOCHROME *c* OXIDASE

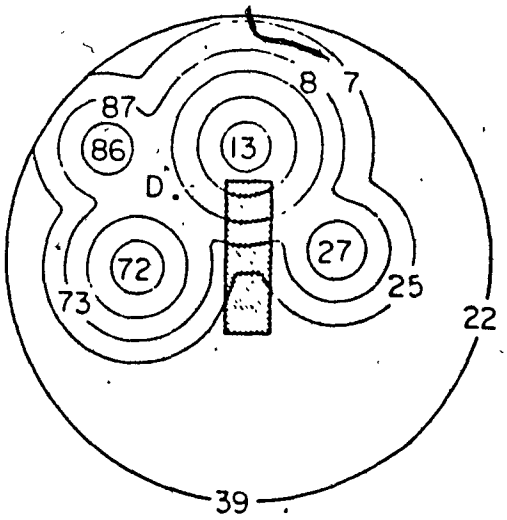

SULPHITE OXIDASE

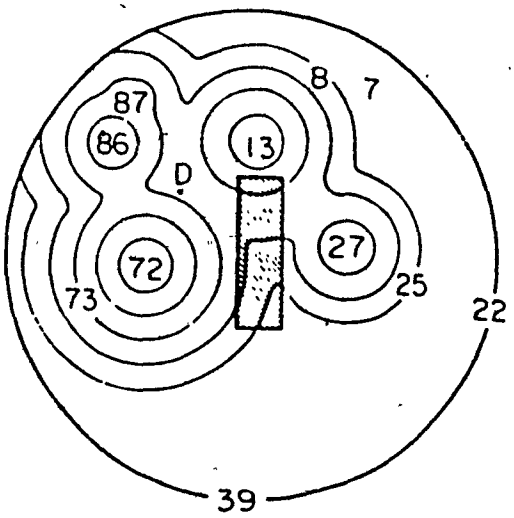

CYTOCHROME *c* PEROXIDASE

past ten years have seen the emergence of a school of thought recognizing that the interplay of protein structure and metal properties were of paramount significance and that the only hope of dealing with the question of electron transfer was to define a new goal for haem protein biochemistry, i.e the understanding of how interactions between the protein and the iron porphyrin determine function.

Protein crystallography and binding studies have provided much information about the interaction domains of electron transfer couples. From these studies has emerged the distinction between reactions involving a short distance between partners (< 10 Å) and those occuring between partners separated by longer distances (>10 Å). In the short distance case, both donor and acceptor haem edges are accessible at the protein surface (e.g.the coplanar haems of the cytochrome b_5:cytochrome c couple with an edge to edge distance of 8 Å) and both partners are electron carriers. In the long distance case, at least one haem is not directly accessible (e.g the cytochrome c peroxidase :cytochrome c couple with haem edges some 18 Å apart) and the acceptor is an enzyme [Poulos, 1984].

The cytochrome c:cytochrome c oxidase couple is another example of a long range electron transfer couple. But unlike the previous example - which features partners with known crystal structures - the x-ray structure of the oxidase

FIGURE 1.4

HAEM a - Cytochrome c oxidase has two such haems. The porphyrin has an α-hydroxyfarnesylethyl group at position 2 of the porphyrin ring, a vinyl at position 4, propionic acids at 6 and 7, a formyl at 8 and methyls at positions 1, 3 and 5. The structure is roughly planar, 8.5 A long and 4.5 A thick [Caughey, 1975]

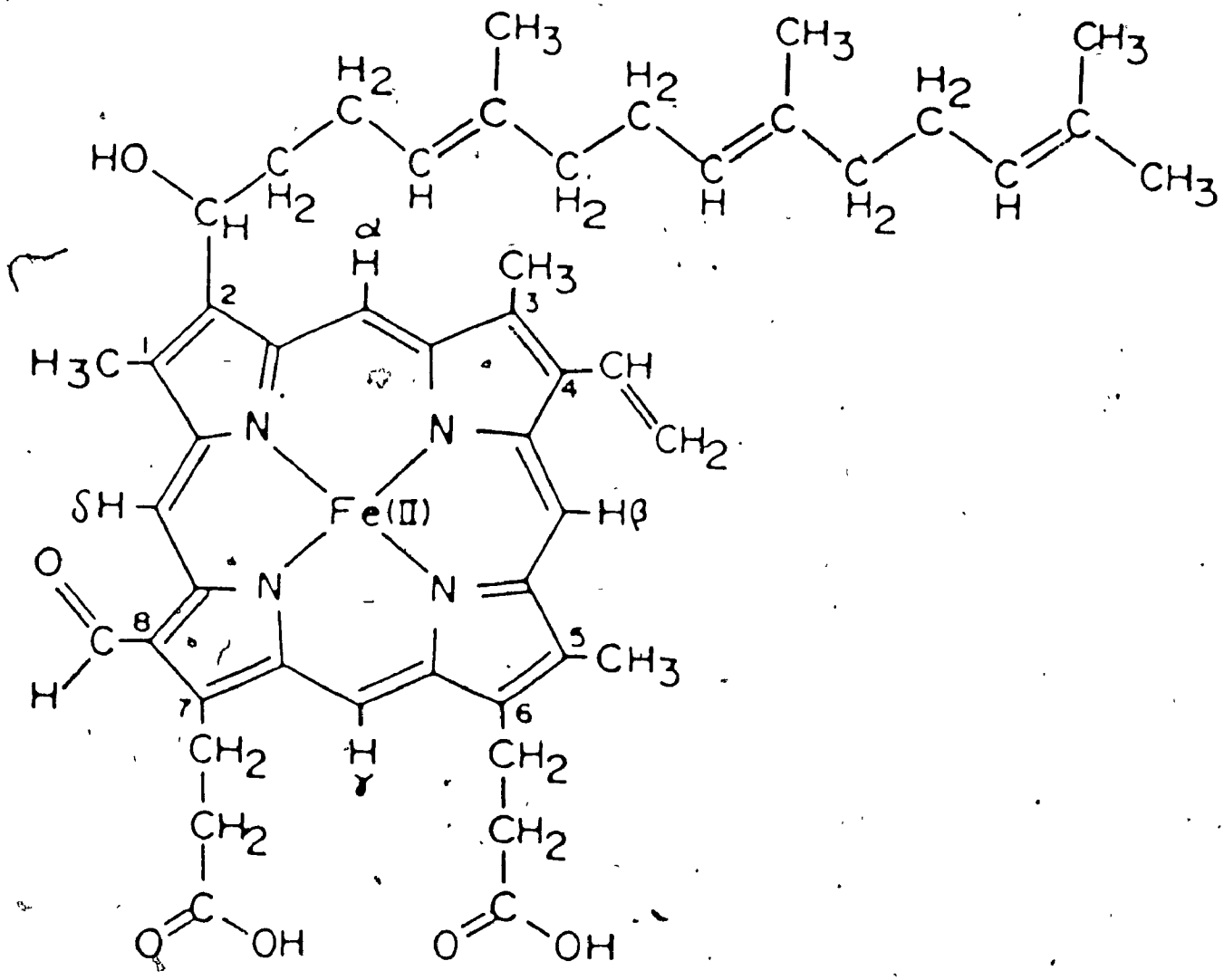
CH3
CH3
CH3
H2
H2
H2
HO
CH
CH2
CH
CH2
CH
CH2
CH
CH2
CH
CH3
α
H
CH3
2
3
1
H3C
CH
4
CH2
N
N
SH
Fe(II)
Hβ
O
N
N
C
8
5
CH3
H
7
6
CH2
H
CH2
γ
CH2
CH2
C
C
O
OH
O
OH

oxidase is unknown, and there is still considerable uncertainty as to its structure-function relationships.

The enzyme is the terminal acceptor in the mitochondrial electron transport chain and it catalyzes the four-electron reduction of dioxygen to water coupling the energy released by the reaction to the synthesis of adenosine triphosphate via a protpn-pumping mechanism across the membrane. It contains four metal sites, two haem *a*'s (Fig 1.4) and two coppers per monomeric unit ($aCu_A a_3 Cu_B$). The two haems and the two coppers are not equivalent: they function differently and are in different protein environments. Cytochrome a_3 and Cu_B together form the dioxygen or extraneous ligand binding centre. Electrons are believed to enter the macroenzyme via haem *a* to be transferred intramolecularly to Cu_A and then to the a_3:Cu_B centre. The oxidase contains anywhere from 7 to 13 subunits for a combined molecular weight of some 200,000. Subunits I and II are the haem-carrying subunits with subunit II additionally bearing the two copper atoms and the cytochrome *c* binding site. The proton-pumping activity has been linked to subunit III. The function of the other subunits is unknown. The oxidase is embedded in and spans the inner mitochondrial membrane as illustrated in Fig 1.5. As such, the monomeric unit constitutes the smallest catalytically active unit [Wikström,1981]. It has also been suggested that the enzyme may be dimeric as shown in the model presented in Fig 1.6, which has led to the conclusion

FIGURE 1.5

[A] SCHEMATIC REPRESENTATION OF A MITOCHONDRIA - It consists of three domains: the matrix within the inner mitochondrial membrane, the intercristal space between the inner and the outer membranes and the cytoplasm outside the mitochondria.

[B] ENLARGEMENT OF [A] - The enzyme protrudes about 50 - 60 A from the membrane on the cytoplasmic side (C) and two small protein domains extend some 10 - 15 A on the matrix side (M).[Brudvig,1981]

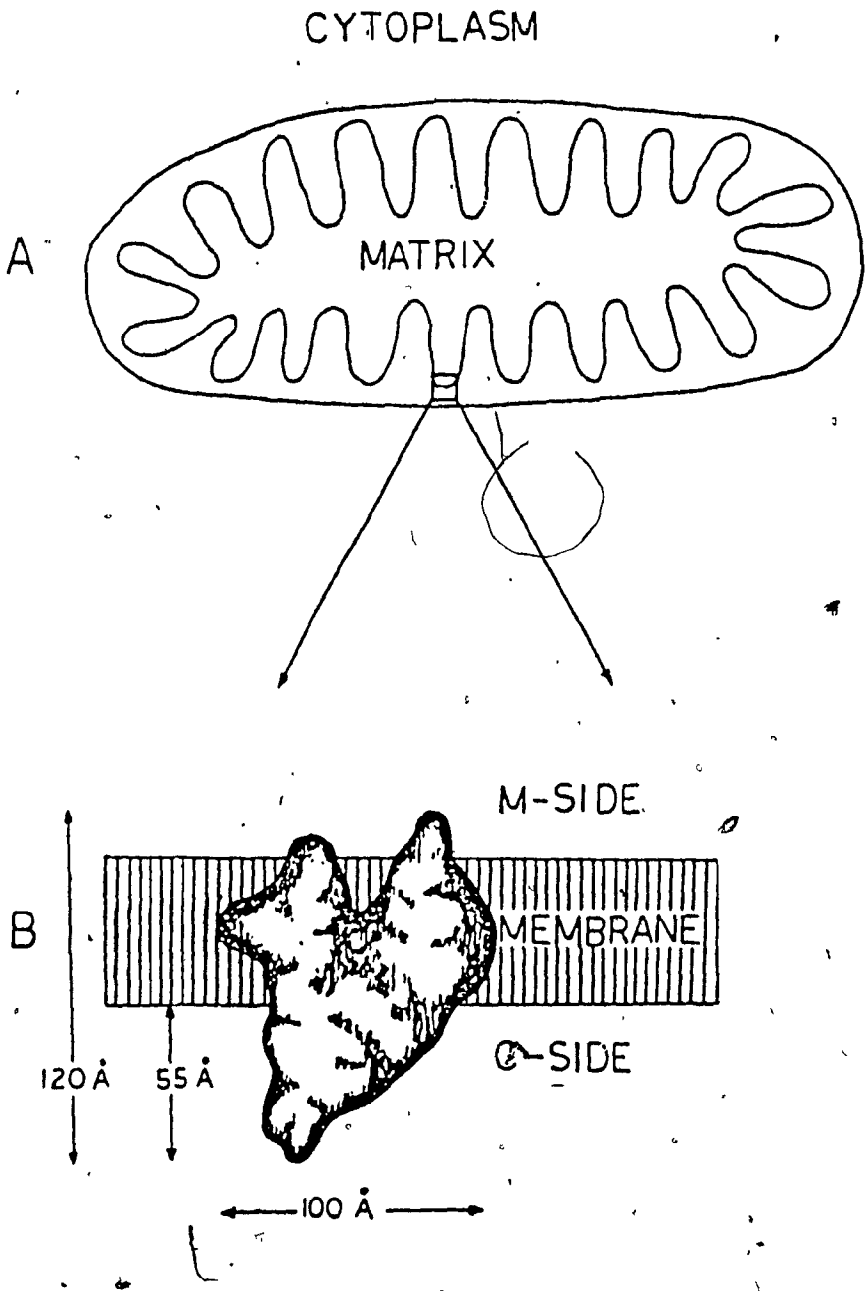
CYTOPLASM
A
MATRIX
M-SIDE
B
MEMBRANE
C-SIDE
120 Å
55 Å
100 Å

FIGURE 1.6

THREE-DIMENSIONAL MODEL OF THE CYTOCHROME OXIDASE DIMER - Electron microscopy and image reconstruction of membraneous crystals confirm that the enzyme protrudes some 60 A on the C side and some 15 A on the M side. Sections through the map are shown parallel to the membrane. The upper five rectangles are spaced by 10 A and show sections of the density map across the dimer.[Deatharage, 1982]

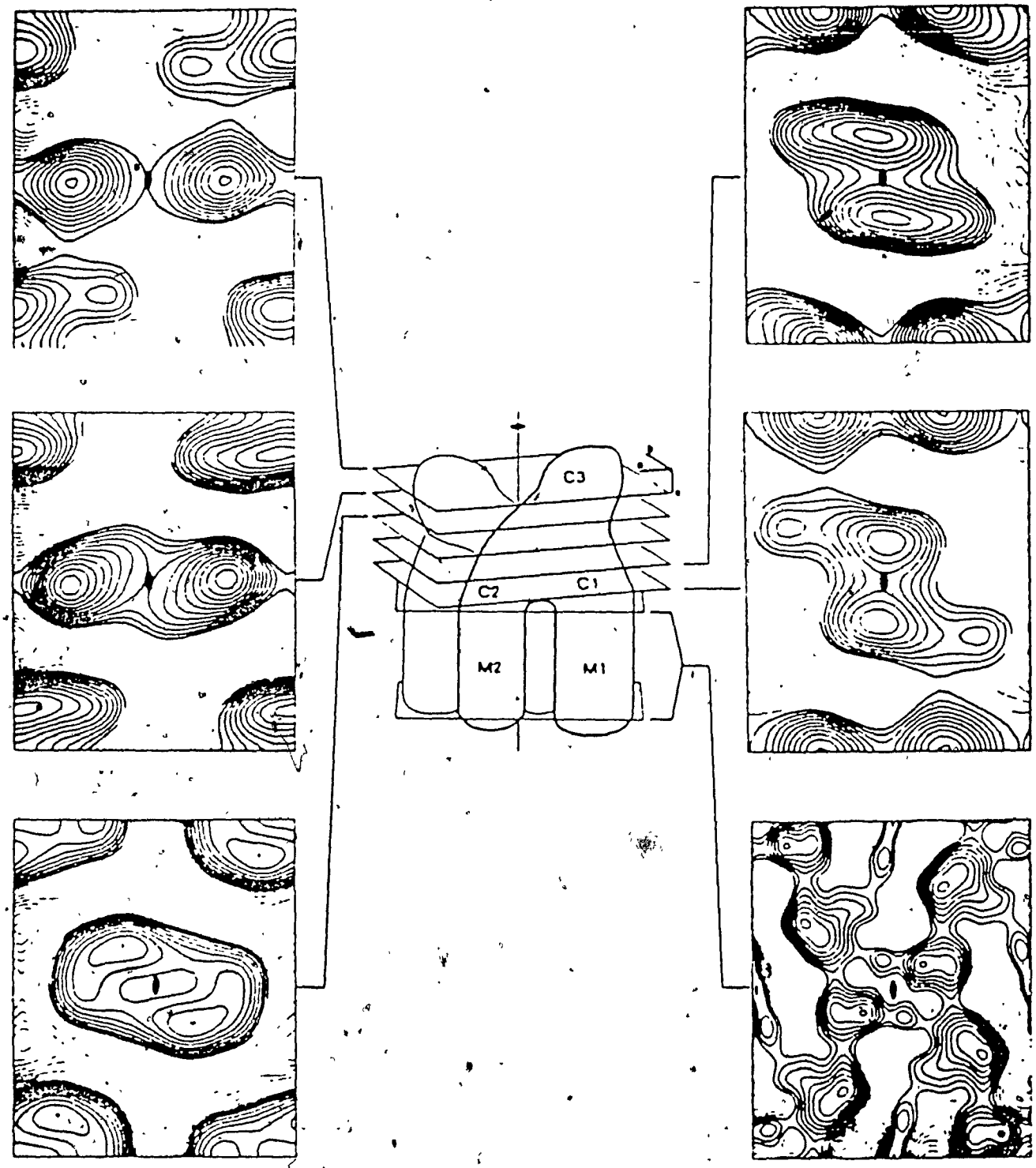
C3
C2
C1
M2
M1

that the oxidase either functions as an $aCu_A a_3 Cu_B$ monomer in which case it would transfer four electrons from cytochrome c to dioxygen or as a $(aCu_A a_3 Cu_B)_2$ dimer, in which case each monomer would transfer two electrons from cytochrome c to each atom of dioxygen [Wainio, 1983].

That the oxidase constitutes one of the most complex biochemical systems should now be apparent, if only for the fact that electron transfer occurs both intermolecularly, between ferrocytochrome c and the oxidase as well as between the oxidase and dioxygen, and intramolecularly between the metal centres. It should be noted that the distinction between these types of electron transfer is far from straightforward. For instance, if cytochrome c and the oxidase exist as a protein-protein complex for a significant amount of time, the reaction may be considered intramolecular...And what about protein fluctuations ? Can they favour conformational changes allowing long range protein complexes to become short range ? These questions are only beginning to be answered. And although much remains to be investigated on the effects of protein-protein interaction on the mechanisms of electron transfer, the information that is now available is being put to use in the design of experiments targetting ever more specific answers. Among the several approaches used to study these questions, a standard experimental design in the haem protein field has been to use metalloderivatives, the strategy being

to replace the iron haem by other metals, such as manganese, copper, cobalt, nickel, tin, zinc , basically by anything that will incorporate into the porphyrin hole and provide the experimenter with a probe otherwise unavailable in the native haem protein. The purpose of this study was to prepare two known closed-shell metal derivatives of cytochrome c by substituting Zn, which is 2+ charged, and Sn, which is 4+ charged, for the haem iron as well as to attempt synthesis of a new cytochrome c derivative, incorporating Eu(III) ion into the porphyrin. Lanthanide porphyrin probes of haem proteins constitute a field of research so new that no group has yet reported incorporation of a rare earth ion into haem. As stated above, the substitution in haem proteins of first row transition metals for iron has allowed the study of structure-function relationships by physical methods not applicable to the native protein. Owing to their sharp electronic properties, lanthanide ions represent environmental probes potentially even more versatile than transition metals. [Richardson, 1982].

The Zn and Sn derivatives exhibit both fluorescence and phosphorescence - quenched in native cytochrome c- thus providing an approach to study both electron and energy transfer processes to the oxidase. The derivatives were then characterized and one of them, the Zn-derivative, was used to attempt photoinduced electron transfer to the oxidase, an investigation never before attempted.

REFERENCES

Brudvig, G.W., Distribution of the Metal Centers in Cytochrome c Oxidase; Thesis, CalTech, 1981. UMI-8104669.

Campbell, I.D.; Dobson, C.M. and R.P.J. Williams, Biochem., 231, 1 (1985).

Caughey, W.S.; Smythe, G.A.; O'Keefe, D.H.; Maskasky, J.E. and M. L. Smith, J. Biol. Chem., 250, 7602 (1975).

Conklin Taylor, K. and G. McLendon, J. Am. Chem. Soc., 110, 3345 (1988).

Deatherage, J.F.; Henderson, R. and R.A. Capaldi, J. Mol. Biol., 158, 501(1982).

Hughes, M.N. The Inorganic Chemistry of Biological Processes, J. Wiley & Sons, New York, 1984.

Koppenol, W.H. and E. Margoliash, J. Biol. Chem., 257, 4426 (1982).

Marcus, R. J. J., Chem. Phys., 24, 966 (1956).

McLendon, G., Acc. Chem. Res., 21, 160 (1988).

Miller, J.R., Science (washington, D.C.), 189, 221 (1975).

Poulos, T.L. and B.C. Finzel, Protein Peptide Rev.; Hearn, M.T. W., Ed.; Marcel Dekker Inc.; New York, 1984, Vol. 4, pp 115-171.

Richardson, F.S., Chem. Rev., 82, 541 (1982).

Salemme, F.R., Am. Rev. Biochem., 46, 299 (1977).

Wainio, W.W., Biol. Rev., 58, 131 (1983).

Wikström, M.; Krab, K. and M.Saraste, Cytochrome Oxidase - A Synthesis; Academic Press, London, 1981.

2.A SHORT PRIMER ON THEORY

2.1 ELECTRON TRANSFER

The major problem with long-range biological electron transfer is that no theoretical formalism yet successfully accounts for it. In solution, electron transfer is something like a random collision process if one considers that the factors of importance are the sizes of the ions, the effect of other ions present in solution and that of solvent. On the other hand, solid state band theory constricts electron transfer to the periodicity -and directionality- of the solid structure. It is essentially a short range propagated phenomenon. Biological electron transfer, we now know, simply does not reduce to a solution problem nor to a solid-state one.

When an electron is transferred between two metalloproteins, the redox sites are more often than not separated by a condensed phase of protein matrix and parameters other than those governing electron transfer, say, between small inorganic ions and single-site metalloproteins - which are readily accounted for by the "inner-sphere/outer-sphere" formalism - become crucial. Additional considerations must be dealt with, and these include the long, non-periodic, distances , the nature of the intervening medium (Is a protein a liquid-crystal ?) as well as the role of fluctuations. On this latter point, it is known that fluctuations in the structure of proteins are

TABLE 2.1: Long-range Biological Electron-transfer Couples

Proteins	Distance(A)		Reference
* Cytochrome c:cytochrome c oxidase			
" :to Cu	18		Glatz, 1979
" :to haem a	25	C	Dockter, 1978
" :to haem a	35	C	Vanderkooi,1977
* Cytochrome c:cytochrome c peroxidase	16.5	E	Poulos, 1980
* Cytochrome c:cytochrome b_2	18	C	Vanderkooi,1980
* Cytochrome c:cytochrome b_5	8.4	E	Salemme, 1976
	18	C	

E = haem edge to haem edge distance

C = metal centre to metal centre distance

commonly involved in tyrosine or phenylalanine ring flips or in haem spin state changes, to name but two examples. What is highly significant is that these are of the order of nanoseconds up to minutes. i.e capable of bearing on electron transfer probabilities [Cooper, 1976]. At present, there is no satisfactory electron transfer theory that successfully deals with the large distances involved (>10 A) in known long-range metalloprotein couples (cf. Table 2.1) and none of the more polished, well-known formalisms take fluctuations into account. As an example for the need to work fluctuations in the theoretical framework are the recent, startling results of Isied *et al.* showing that electron transfer rates are dependent on the direction of transfer [Bechtold, 1986]. This not only implies irreversibility but also that different microstates are possibly involved in oxidation and reduction [Williams, 1986].

Classical treatment [Marcus, 1980], rests on the Franck-Condon principle which requires that nuclear coordinates remain essentially unchanged during the electronic transition, i.e if they are to rearrange, they must do so before electron transfer. The treatment considers as negligible the probability of electron transfer occurring between reactants that are far apart, as illustrated in Fig 2.1 Adiabatic processes are those of ordinary chemical reactions in which chemical bonds are broken or remade. But 95% of biological electron transfer processes are

FIGURE 2.1

[A] POTENTIAL ENERGY OF A SYSTEM OF REACTANTS AND ENVIRONMENT(R) AND PRODUCTS WITH ENVIRONMENT(P) VS. NUCLEAR COORDINATES OF THE SYSTEM - The plot is made for the case of no electronic interaction between reactants that are far apart. The system on R remains on that surface no matter what fluctuations the nuclear coordinates undergo.
[B] SAME AS [A] FOR THE CASE OF ELECTRONIC COUPLING BETWEEN REACTANTS. A fluctuation of nuclear coordinates allows the R system to cross over to the P surface as it goes through the intersection region. When the splitting is large, the electron transfer probability is unity if the system has enough thermal energy to overcome the barrier and it is called ADIABATIC. This is never the case with biological electron transfer: the long distances between reactants decreases their interaction energy and very few trajectories will lead the system to the P surface [Marcus, 1979]. In quantum mechanical treatments, tunneling through the barrier is allowed.

NON-ADIABATIC:

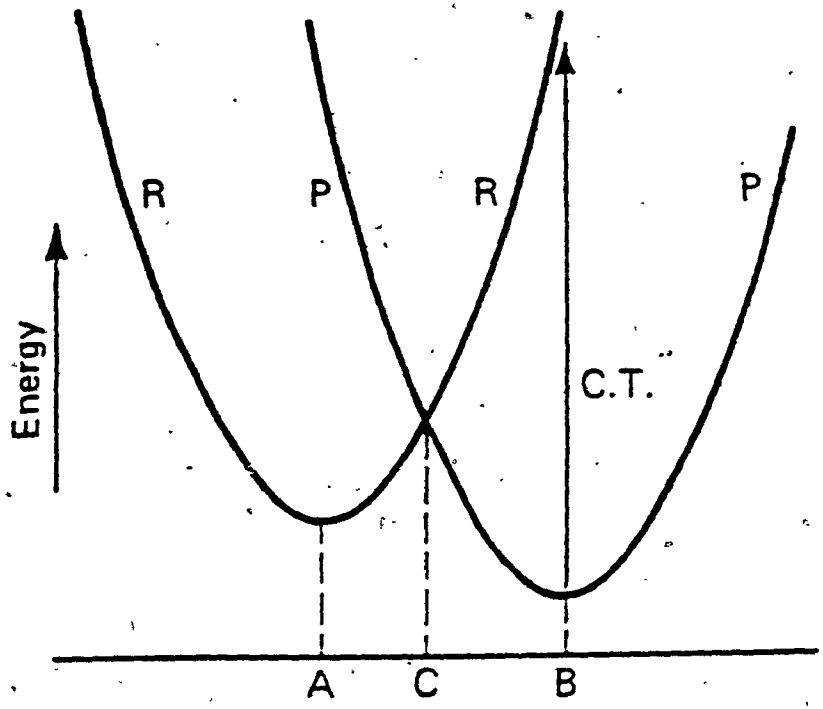

Nuclear Coordinate

(A)

ADIABATIC:

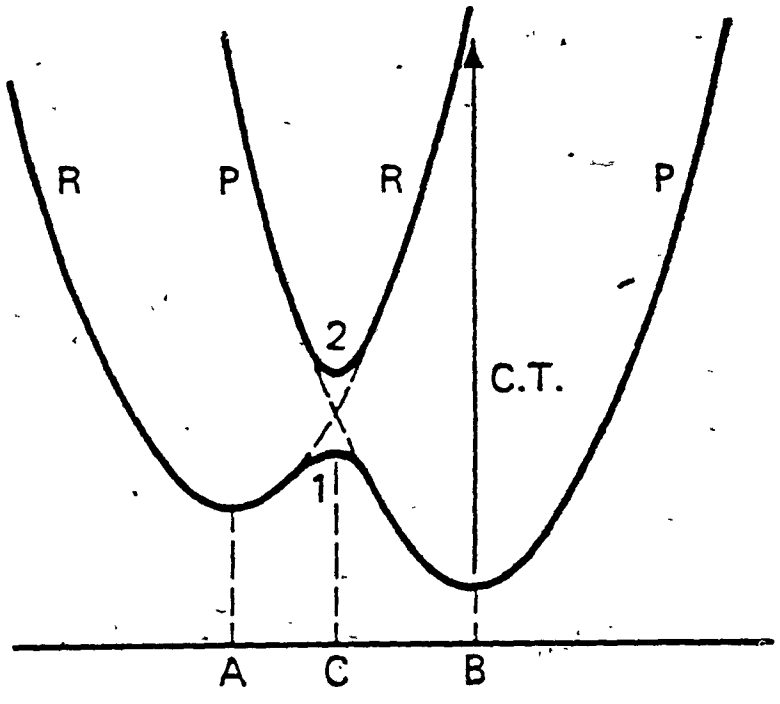

Nuclear Coordinate

(B)

non-adiabatic, i.e. most trajectories along the PE surfaces will proceed up the R surface and electron transfer again has a low probability. Semiclassical approaches include Hopfield's tunneling formalism [Hopfield, 1974] which has two major drawbacks: first, it rests on the premise that the process is occurring between sites of fixed geometry, therefore that they are independent from each other as implied by his treatment which uses separate spectral functions for each site; second, it predicts too a very low probability of electron transfer between sites separated by more than 10 Å. and fails to account for electron transfer rates observed at low temperatures. Jortner's treatment [Jortner, 1976] has the advantage that it is concerned with the response of the entire system to the exchange of charge. By considering the role of high-ν multiphonon modes, it thus provides for a dynamic approach where each site has its own function.

It successfully accounts for the low temperature rates but I have yet to come across a clear exposition of any sort of solution to the long distance problem, in spite of Jortner's claim that "the non-adiabatic case is easily soluble"...[1] In recent years, the problem has received increased attention from experimentalists as well. Mentioned earlier (V. Introduction) were some of the significant contributions dealing with crucial physical parameters. This is the point where the distinction between inter- and intramolecular

electron transfer becomes very pertinent [Scott, 1985]. Consider the following:

$$A + D \underset{}{\overset{K_p}{\rightleftharpoons}} A{:}D \xrightarrow{K_{et}} A^+{:}D^- \underset{K_s}{\rightleftharpoons} A^+ + D^- \qquad (2.0)$$

where A is the electron acceptor and D the donor. In the intermolecular case, K_p and K_s are association constants for the precursor ($A{:}D$) and successor ($A^+{:}D^-$) complexes. Electron transfer occurs between them with rate K_{et}. The rate of intramolecular electron transfer only depends on factors which influence K_{et} while that of intermolecular electron transfer is also affected by factors influencing the formation of the precursor complex, such as diffusion (both in solution and in/out of a membrane) and electrostatic interactions. These considerations have led experimentalists to investigate intramolecular electron transfer systems which require only having to deal with K_{et}. The experiments then simplify to the investigation of the factors which have a direct bearing on K_{et}, namely: the distance between the redox sites within the complex, the driving force of the electron transfer process, the nature of the intervening phase of protein and the relative orientation of the redox sites. Two approaches are now used to ensure that the system will reduce to the simplified intramolecular case. The first approach consists in using a structurally well-characterized protein containing a haem redox center and covalently attaching a

small inorganic complex to a surface protein residue [Axup, 1988]]. This satisfies the intramolecular condition that the redox sites be fixed relativeto oneanother and enables the definition of intersite distance restrictions for metalloprotein electron transfer while allowing correlations to some of the semiclassical theoretical approaches that are presently favourably considered. The second approach -used in this work- is chemically milder and involves the preparation of protein complexes which have very high formation constants in low ionic strength media [Liang,1986]. They also allow the experimentalist to work in the "intramolecular limit" while being closer to the elusive objective of direct observation of electron transfer over distances greater than 10 A.

2.2 ENERGY TRANSFER

In this work, energy transfer is of interest as it constitutes a possible mode of transferring charge from a protein donor to an acceptor, i.e as a process competing with electron transfer in the long range context and for its use as "spectroscopic ruler" [Stryer, 1982] to evaluate donor-acceptor distances in the 20-80 A range.

The radiationless transfer of electronic excitation energy frequently proceeds via one of two fundamental mechanisms: inductive-resonance or exchange-resonance. In the former case, the interaction of an excited energy donor with an unexcited acceptor occurs via electromagnetic fields. The

quantum-mechanical theory of this type of radiationless energy transfer by dipole-dipole interaction between a pair of donor and acceptor chromophores was developed by Förster [Förster, 1951]. The expression defining the rate constant for energy transfer by this mechanism between a donor D^* and an acceptor A at a distance R is:

$$k_T = k_o(R/R_o)^{-\sigma} \qquad (2.1)$$

where k_o is the rate constant for emission by the donor in the absence of energy transfer. R_o is the "critical radius", distance between D^* and A at which the probability of energy transfer is just equal to the sum of the probabilities for all de-excitation processes of D^*. It is given by:

$$R_o = (JK^2\phi_o n^{-4})^{1/\sigma}\ (9.79 \times 10^3) \qquad (2.2)$$

where J represents the spectral overlap integral (in cm^3M^{-1}). K^2 is a dimensionless orientation factor of order one, ϕ_o is the quantum yield of the donor in the absence of energy transfer and n is the refractive index of the medium. The overlap integral is given by:

$$J = \left[\int_o^\infty \varepsilon_A(\lambda) \cdot f_D(\lambda) \cdot \lambda^4 \, d\lambda \right] / \int_o^\infty f_D(\lambda)\, d\lambda \qquad (2.3)$$

where $\varepsilon_D(\lambda)$ is the extinction coefficient of the acceptor ($cm^{-1}M^{-1}$) and $f_D(\lambda)$ is the relative emission intensity of the donor per unit wavelength interval. Donor emission decays exponentially with a lifetime given by:

$$\tau = (k_o + k_T)^{-1} \qquad (2.4)$$

and the transfer efficiency, E, represents the fractional decrease in emission due to energy transfer. It is expressed

as follows:

$$E = k_T/(k_T + k_o) = 1 - \tau/\tau_o \qquad (2.5)$$

in which : $\tau_o \triangleq 1/k_o$ (2.6)

In order to determine the distance R between donor and acceptor, the lifetime or quantum yield of the donor in presence and in absence of the donor are measured and J is calculated. In most cases, it is the determination of R_o which limits the accuracy of the distances obtained, chiefly due to the uncertainty in the value of K^2 [Steinberg, 1971]. Theoretically, K can range between 0 and 4 , but structural molecular considerations allows one to considerably narrow the range of possible values, thus increasing the accuracy of the determined distance [Vanderkooi, 1980].

The inductive-resonance energy transfer process depopulates the electronically excited state of the donor and directly competes with radiative and radiationless de-excitation processes. It occurs as a result of dipole-dipole, coulombic interactions which couple the initial (D^*A) and final (DA^*) states of the system. Essentially a long range phenomenon as it proceeds over distances greater than collisional diameters, it contrasts sharply with the exchange-resaonance mechanism, which is a short range process requiring overlap of electron clouds and featuring the addition of an exchange term to the coulombic interaction. The formula describing the rate of energy transfer via the exchange mechanism is:

$$k_{T(ex)} \propto \exp(-2R/L) \int_{0}^{\infty} f_D(\bar{\nu})\ \varepsilon_A(\bar{\nu})\ d\bar{\nu} \qquad (2.7)$$

where L is the effective Bohr radius. This rate can also be expressed by a simplified form of the Debye formula :

$$k_{T(ex)} \propto 8RT/3{,}000\ \eta \qquad (2.8)$$

in which η represents the viscosity of the medium.

REFERENCES

Axup, A.W.; Albin, M.; Mayo, S.L.; Crutchley, R.J. and H. B. Gray, J. Am. Chem. Soc., 110, 435 (1988).

Bechtold, R.; Kühn, C.; Lepre, C.and S. Isied, Nature, 322, 286 (1986).

Cooper, A., Proc. Natl. Acad. Sci. USA , 73, 2749 (1976).

Dockter, M.E.; Steineman, A. and G. Schatz, J. Biol. Chem., 253, 311 (1978).

Förster, T., Fluoreszenz Organisher Verbindungen, Vandenhoeck & Ruprecht, Göttingen, 1951.

Glatz, P.; Chance, B. and J. M. Vanderkooi, Biochem., 18, 3466 (1979).

Hopfield, J.J., Proc. Natl. Acad. Sci. USA, 71, 3640 (1974).

Jortner, J., J. Chem. Phys., 64, 4860 (1976).

Liang, N.; Kang, C.H.; Ho, P.S.; Margoliash,E. and Hoffman, B., J. Am. Chem. Soc.,108, 4665 (1986).

Marcus, R. A., Tunneling in Biological Systems; Chance, B.;DeVault, D.C.; Frauenfelder, H.; Marcus, R.A.; Schrieffer, J. R.; Sutin, N. Eds; Academic Press, New York, 1979, pp 109-125.

Scott, R. A.; Mauk, A. G. and H. B. Gray, J. Chem. Educ., 62, 932 (1985).

Stryer, L.; Thomas, D.D. and C. F. Meares, Ann. Rev. Biophys. Bioeng., 11, 203 (1982).

Vanderkooi, J. M.; Landersberg, R.; Hamden, G.W. and C.S. Owen, Eur. J. Biochem., 81, 339 (1977).

Vanderkooi, J. M.; Glatz, P.; Casadei, J. and G. V. Woodrow, Eur. J. Biochem., 110, 189 (1980).

Williams, R.J.P. and D. Conacr, Nature, 322, 213 (1986).

NOTE

1 - See the general discussion on "Formulation of Theory" in Tunneling in Biological Systems (ref. v. supra) pp 95-105.

3. BACKGROUND

3.1 THE TRIPLET STATE

It is generally agreed that the lowest excited states of most porphyrins and metalloporphyrins are π,π^* states, with the electronic excitation localized on the macrocycle. The central metal can exert significant perturbation on the excited states, affecting such properties as electron-donating or electron-accepting capacity, as well as their radiative decays. Their singlet solution spectra are characterized by an intense band - the Soret or B band - near 400 nm ($\varepsilon \simeq 200$ $mM^{-1}cm^{-1}$) corresponding to a fully allowed transition and two weaker transitions ($\varepsilon \simeq 30$ $mM^{-1}cm^{-1}$) around 550 nm - the α and β or Q_o and Q_v bands -. Vibronic fine structure is not observed [Makinen,1983].

Porphyrins make ideal photosensitizing agents due to the relatively small energy gap between the lowest singlet and triplet states. Common singlet and triplet energies for metalloporphyrins are in the 47 and 43 kcal/mol range, respectively [Hopf, 1978]. Singlet lifetimes are in the nanosecond regime and triplet lifetimes are often in the millisecond timescale. Electron and energy acceptors quench the excited states of porphyrins and the corresponding rate constants of course depend on the electron donor and electron acceptor properties of the reactants. Direct observation of singlet/triplet excited state quenching phenomena are most

FIGURE 3.1

JABLONSKI DIAGRAM ILLUSTRATING SINGLET AND TRIPLET STATES - Metalloporphyrins are excellent photosensitizers due to their strong ultraviolet and visible absorption spectra, small singlet-triplet splittings and high intersystem crossing efficiencies.

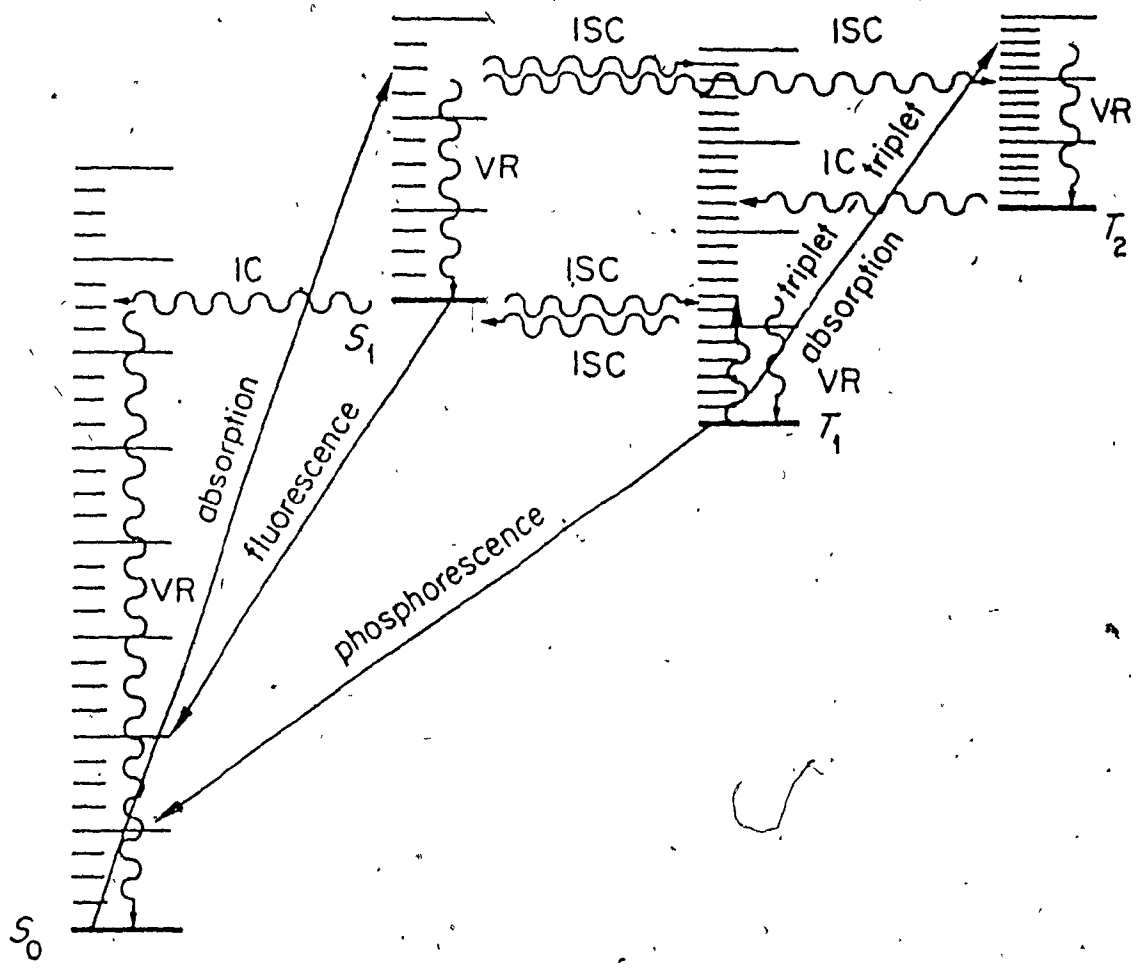
ISC
ISC
VR
IC
triplet
VR
IC
ISC
triplet
absorption
ISC
S_1
T_2
absorption
fluorescence
VR
T_1
phosphorescence
VR
S_0

conveniently made by laser or flash photolysis methods by pulse excitation and measurement of the decay of the transient absorption/emission.

In an excited state quenching phenomenon, the basic processes are as follows:

$$D \xrightarrow[I_a]{h\nu} D^* \qquad (3.1)$$

$$D^* \xrightarrow{k_e} D + h\nu \qquad (3.2)$$

$$D^* \xrightarrow{k_q} D + \Delta \qquad (3.3)$$

$$D^* + Q \xrightarrow{k_z} D + Q^*$$

$$\text{"} \quad \text{"} \quad D^+ + Q^-$$

$$\text{"} \quad \text{"} \quad D^- + Q^+ \qquad (3.4)$$

where D is the donor, D^* the excited donor, and Q a quencher. Steps 3.2 to 3.4 represent the possible deactivation pathways for D^*. k_e is the first-order rate constant for the emission of light from D^*, k_q is the sum of all first- or pseudo first-order rate constants for deactivation of D^* and k_z is a bimolecular rate constant accounting for the diffusional deactivation of D^* by Q. Equation 3.4 shows that quenching may be due to energy transfer, or to reductive/oxidative electron transfer. In the case of fixed site donor-acceptors, i.e. in the diffusion-free intramolecular limit, k_z is first-order. In metalloporphyrins, singlet and triplet lifetime decays occur on such different timescales that the two processes need not be deconvoluted. Both reductive and oxidative quenching has been reported in these systems with

the most studied electron transfer process being that by electron acceptors [Hopf, 1978]. In polar solvents, singlet and triplet quenching by electron acceptors generally produce free ions which recombine with back electron transfer to yield ground states of the starting reactants.

3.2 RELATIONSHIP TO EXISTING RESEARCH

3.2.1 CYTOCHROME c METALLODERIVATIVES

J. Vanderkooi's group was the first to attempt incorporation of closed-shell metals into cytochrome c for the purpose of using them as fluorescent and phosphorescent probes in haem protein structure-function studies. Sn^{4+} and Zn^{2+} cytochrome c were successfully synthesized starting from porphyrin cytochrome c - the iron-free derivative of the native protein - and the respective metal salts. In subsequent work [Vanderkooi, 1977], the same group used the derivatives to characterize the cytochrome c binding site. They established that the derivative binding site to cytochrome c oxidase was the same as that of native cytochrome c and that their affinity for the oxidase was comparable to that of cytochrome c. They also observed that the fluorescence of Znc was quenched by the oxidase which allowed them to eliminate electron/energy transfer mechanisms requiring close contact between the haems. In further work, Dixit *et al.* observed and measured the decay time of the transient triplet absorption and emission of Znc, reporting lifetimes of 14 msec for both processes, a λ_{max} of 462 nm for absorption and

720 nm for emission [Dixit, 1981], as well as quantum yields for fluorescence [ϕ_f Snc = 0.012; ϕ_f Znc = 0.055], phosphorescence [ϕ_p Snc = 0.0043; ϕ_p Znc = 0.0044], efficiency values for triplet formation [Snc = 0.95; Znc = 0.9], fluorescence lifetimes [τ_fSnc = 1 nsec; τ_f Znc = 3.3 nsec] as well as phosphorescence lifetimes [τ_p Snc = 0.005 sec; τ_p Znc = 0.014 sec].[Dixit, 1984].

In this part of the work, synthesis of the same derivatives was attempted to provide the laboratory with metallocytochrome c synthesis expertise. The derivatives were meant to be used in singlet as well as triplet studies of the interaction with the oxidase. In addition, the Snc was intended as a suitable Mössbauer probe. Finally, the experience gained with these derivatives was to be used to synthesize the Eu^{3+} species.

3.2.2 Znc IN ELECTRON/ENERGY TRANSFER STUDIES

The finding that ^{3}Znc can be formed in high yield with a remarkably long lifetime prompted research groups to use it as a donor in photoinduced energy/electron transfer experiments. The excited ^{3}Znc is an electronic isomer of the ground state and as such, has chemical properties widely different from the ground state. It has been shown to undergo energy/electrontransfer reactions which alter its lifetime and spectrum.

Four recent research contributions are of interest. The first

FIGURE 3.2

DIFFERENCE SPECTRA OF $^{3}Znc/Znc$ (o) AND OF $Znc/Znc^{\bullet+}$ (Δ) [Elias, 1988]

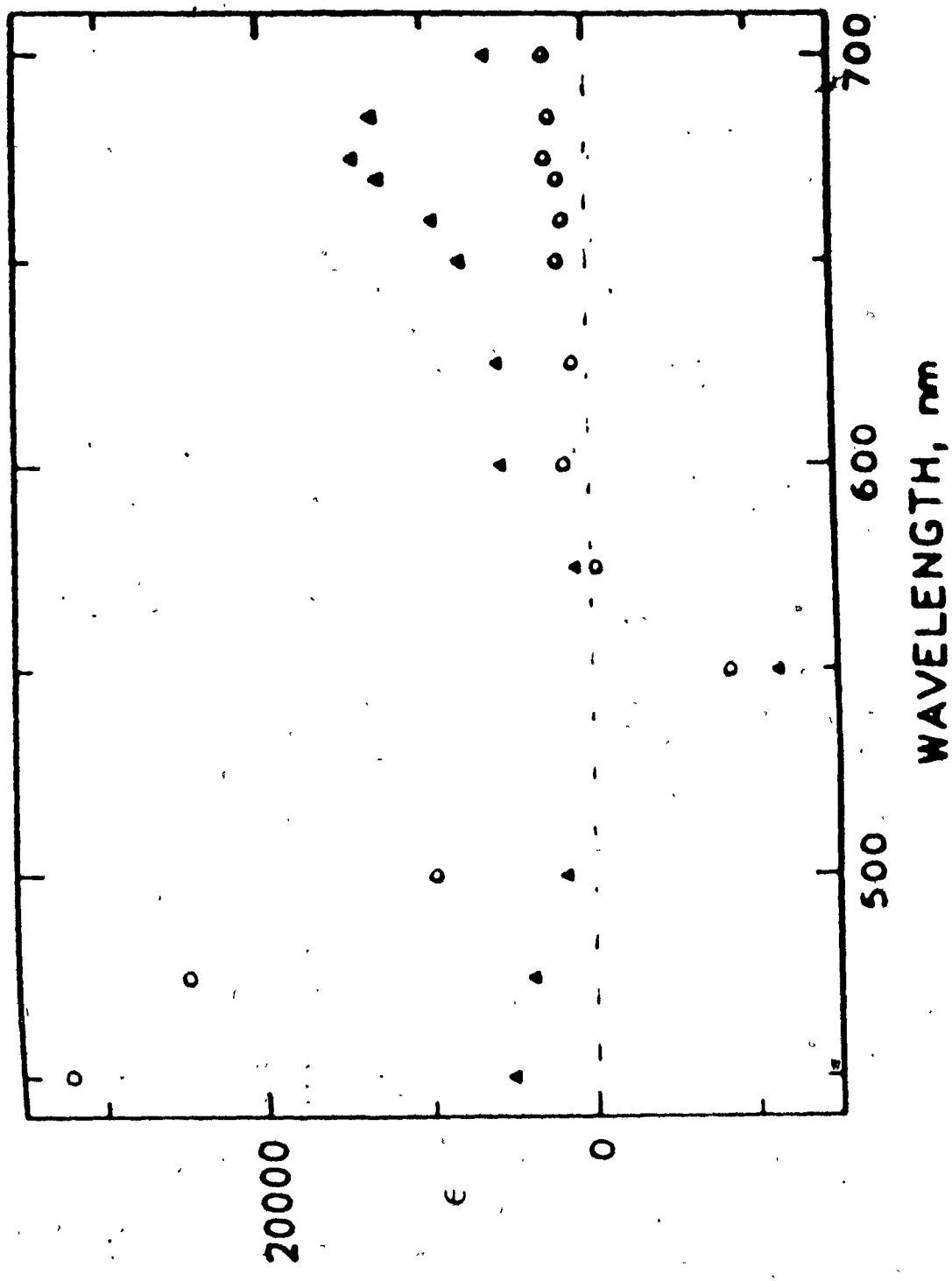
700
600
500
WAVELENGTH, nm
20000
ε
0

deals with the electron transfer kinetics of Zn$\underline{c}$ and its pentaamine his-33 derivative [Elias, 1988]. The ^{3}Zn$\underline{c}$ state was quenched in the presence of the 11.8 A-distant electron acceptor $Ru(NH_3)_5(His)^{3+}$. The triplet was found not to decay back to the ground state but to yield two electron-transfer products: Zn$\underline{c}^{+}$ and $Ru(NH_3)_5(His)^{2+}$. The forward electron transfer rate was 7.7×10^3 s^{-1} and that of the thermal back-reaction was 1.6×10^6 s^{-1}. The authors also published ^{3}Zn$\underline{c}$/Zn$\underline{c}$ and Zn$\underline{c}^{+}$/Zn$\underline{c}$ difference spectra [Fig 3.2].

The second contribution of interest in this context is that of Liang *et al.*.who studied photoinduced electron transfer from two types of ferrocytochrome$\underline{c}$'s (tuna and yeast) to (yeast) ZnCcP within a 1:1 complex [Liang,1986]. The reaction was initiated by photoexcitation of the ^{3}ZnCcP which can decay back to the ground state or reduce the oxidized haem partner:

$$[ZnCcP{:}\underline{c}^{3+}] \underset{k_D}{\overset{h\nu}{\rightleftharpoons}} [^3ZnCcP{:}\underline{c}^{3+}] \xrightarrow{k_t} [ZnCcP^{+}{:}\underline{c}^{2+}] \quad (3.5)$$

The redox intermediate then returns to the ground state by thermal electron transfer from $\underline{c}^{2+}$ to the cation radical $ZnCcP^{+}$:

$$[ZnCcP^{+}{:}\underline{c}^{2+}] \xrightarrow{k_b} [ZnCcP{:}\underline{c}^{3+}] \quad (3.6)$$

The decay of ^{3}ZnCcP within the $[ZnCcP{:}\underline{c}^{3+}]$ complex is first-order with decay rate $k_P = k_D + k_t$. Values of k_P of 140 s^{-1} and 381 s^{-1} were observed for the tuna and yeast complexes, respectively, yielding k_t values of 25 s^{-1} and of 266 s^{-1}, thus showing the increased affinities between

partners from the same organism (yeast). Growth of the redox intermediate [ZnCcP^{+}:c^{2+}] was observed, simultaneous with the ^{3}ZnCcP decay.

The third contribution of interest is the work reported by Zemel and Hoffman on the decay of the excited triplet porphyrins in zinc myoglobin and hemoglobin. They were able to observe triplet energy transfer within the tetrameric structure, in which the haems are some 20 A apart. They considered the two most likely mechanisms for the observed quenching, i.e the inductive or exchange-resonance mechanisms, and finally concluded that the dipole-dipole process should be favoured, due to the short-distance nature of the exchange mechanism [Zemel, 1981].

Finally, McLendon et al. recently described another reaction of ^{3}Znc, that with cytochrome b_5. The authors observed quenching of the triplet in the 1:1 complex (k_P = 5 x 10^5 s^{-1}) and argued in favour of electron transfer as quenching mechanism -although electron transfer products could not be detected - over dipole-dipole energy transfer since Förster formalism yielded a rate of transfer two orders of magnitude greater than the observed rate [McLendon, 1985].

After synthesis of the Zn-derivative, this work proceeded with flash photolysis experiments in the hope of observing similar quenching of ^{3}Znc when complexed to the oxidase.

REFERENCES

Demas, J.N., Excited State Lifetime Measurements; Academic Press, New York, 1983.

Dixit, S.N.; Waring, A.J. and J. M. Vanderkooi, J.M., FEBS Lett., 125, 86 (1981).

Dixit, S.N.; Moy, V.T.and J. M. Vanderkooi, Biochem, 23, 2103 (1984).

Elias, H.; Chou, M.H. and J, R. Winkler, J, Am. Chem. Soc., 110, 429 (1988).

Hopf, F.R. and D. G. Whitten, The Porphyrins; D. Dolphin, Ed.; Academic Press, New York, 1978, Vol. II, Part B, pp 161-195.

Liang, N.; Kang, C.H.; Ho, P.S.; Margoliash, E.and B. Hoffman, J. Am. Chem. Soc., 108, 4665 (1986).

Makinen, M.W.and A. Churg, Iron Porphyrins; Lever, A.B.P.; Gray, H. B. Eds; Addison-Wesley, Reading, Mass., 1983, Part I, pp. 141-235.

McLendon, G.L.; Winkler, J.R.; Nocera, D.; Mauk, M.R.; Mauk, G.A. and H. B. Gray, J. Am. Chem. Soc., 107, 739 (1985).

Vanderkooi, J.M.; Adar, F. and M. Erecinska, Eur. J. Biochem., 64, 381 (1976).

Vanderkooi, J.M.; Landesberg, R.; Hayden, G. W. and C. S. Owen, Eur. J. Biochem., 81, 339 (1977).

Zemel, H. and B. Hoffman, J. Am. Chem. Soc., 103, 1192 (1981).

4. SYNTHESIS OF CYTOCHROME c DERIVATIVES AND OXIDASE COMPLEXES

4.1 IRON-FREE CYTOCHROME c

Iron-free cytochrome c --- porphyrin cytochrome c, c^{-Fe}--- is prepared following the laboratory's standard procedure [Kornblatt, 1984], itself a modification of Robinson and Kamen's method [Robinson, 1968]. In a typical preparation, some 50 mg of cytochrome c (Sigma, Type III) are dried on a vacuum line for ca. one hour. The sample is then briefly exposed to anhydrous HF (ca. 10 sec) and dried overnight on the line.It is dissolved in 10 mM EDTA, pH 6 and at ca. 1 mM, is dialyzed against three changes of the same at 4° C. The sample is then applied to a Sephadex G-75 column. In native cytochrome c, porphyrin fluorescence (ca. 600-700 nm) is quenched by the haem [Fisher, 1973]. Removal of the iron restores the porphyrin fluorescence, thus providing a convenient monitoring tool.

The absorbance of the collected fractions is conveniently monitored at 550 nm to determine cytochrome c elution and their emission at 620 nm -with excitation in one of the porphyrin bands- to determine porphyrin c elution. Only those fractions whose cytochrome c elution comigrates with porphyrin fluorescence are saved [Fig 4.1] and higher molecular weight components are always discarded.The samples are stored at -15° C until further use. Porphyrin c is now routinely used in haem protein structure-function research as it is well established that no other alteration in the

FIGURE 4.1

COMIGRATION OF IRON-FREE CYTOCHROME $\underline{c}$ AND NATIVE CYTOCHROME $\underline{c}$ - A 3 μM $\underline{c}^{-Fe}$ sample in 25 μM cytochrome $\underline{c}$ is chromatographed at 4° C on a 46 x 0.8 cm Ø column of Sephadex G-75 equilibrated in 10 mM EDTA, pH 6 at a rate of 6 $ml\,h^{-1}$. The fluorescence intensity of the fractions is read at 620 nm - maximun $\underline{c}^{-Fe}$ emission - (open circles, dashed lines). The fractions are then reduced with sodium dithionite and $\underline{c}^{+2}$ absorbance is read at 550 nm (closed circles, full line). The elution profile shows presence of higher molecular weight components, usually representing ca. 15% of the sample after dialysis and less than 4% after G-75 chromatography.

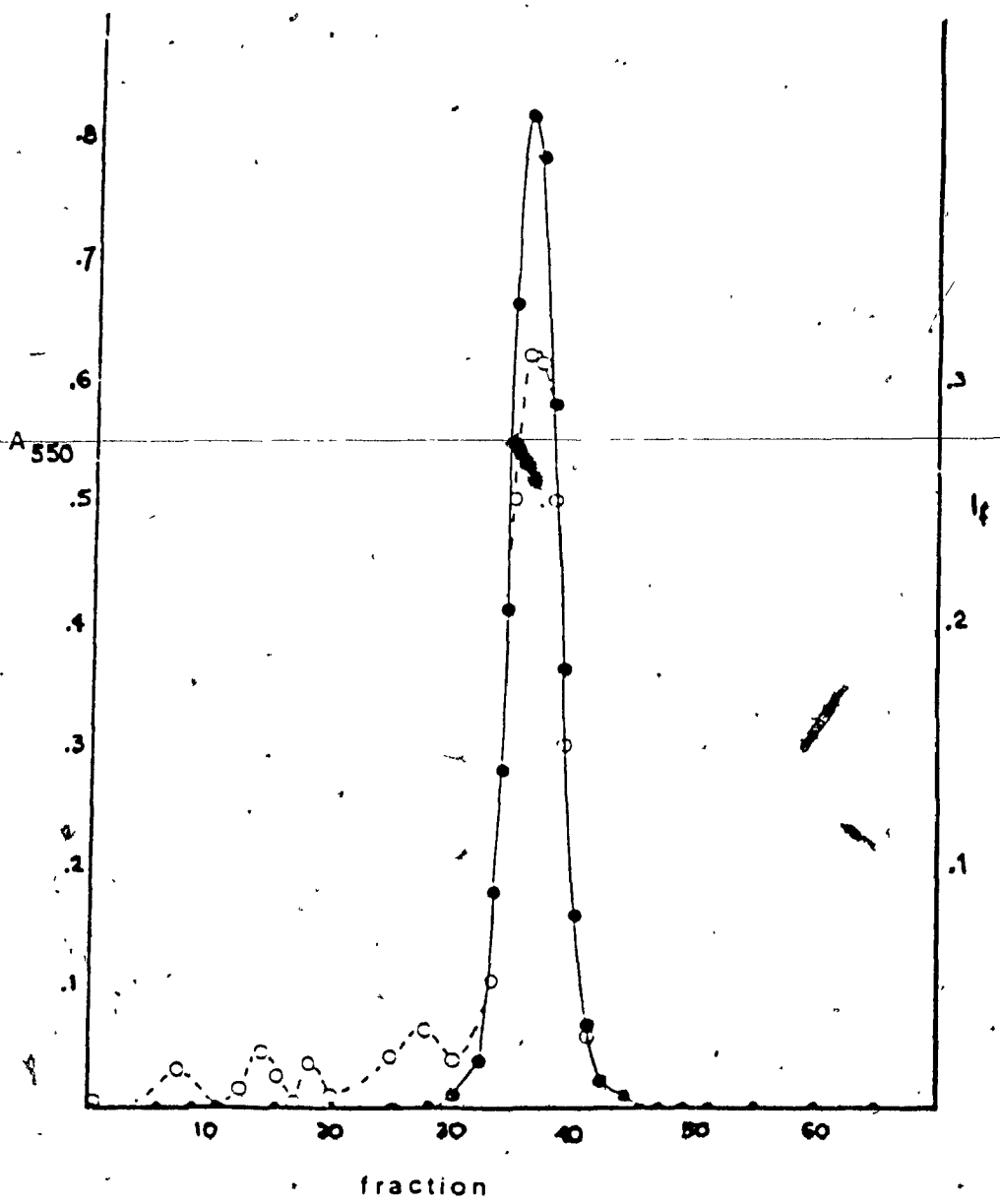
.8
.7
.6
A 550
.5
.4
.3
.2
.1
.3
.2
.1
10
20
30
40
50
60
fraction

primary structure of the protein occurs besides quantitative iron removal [Vanderkooi,1977].

4.2 ZINC CYTOCHROME c

4.2.1 SYNTHESIS

Zinc cytochrome c is prepared by modification of the Vanderkooi method [Vanderkooi, 1976]. Porphyrin c [ca. 250 μM], prepared as in the previous section, is thawed and dialyzed against 20 mM KH_2PO_4. Alternatively, fresh porphyrin c is prepared and the residue taken up in the above solution. Starting with cytochrome c does not lengthen the procedure unduly as almost equivalent time is required to test/chromatograph the frozen c^{-Fe} sample. The dialysate is brought to pH 2.5 with addition of 6 N HAc with stirring. A ten-fold excess of $ZnCl_2$ is added to the mixture which is then placed in a 40° C bath for one hour. The solution is then dialyzed against HAc, pH 3, for 3 hours, followed by a 2-hour dialysis against distilled water. It is then dialyzed against two changes of 20 mM KPi, pH 5. Finally, it is concentrated - and further purified- by ultrafiltration, using a YM 5,000 molecular weight cut-off. The ultrafiltration step is important, as low-molecular weight components are always present. The presence of aggregates or higher molecular weight components was not detected, either by ultrafiltration or by chromatography. Ultrafiltration can

be subsituted by gel filtration as final purification step but the former method has the added advantage of concentrating the protein. Final dialysis is carried out against 5 mM KPi, pH 7, prior to freezing.

4.2.2 CHARACTERIZATION

Fig 4.2 shows the absorption spectrum of Zn$\underline{c}$. As a result of metal insertion, the Soret band sharpens and the $\underline{c}^{-Fe}$ four-band spectrum in the 500-600 nm region collapses into two bands (cf. Fig 4.3). Vanderkooi *et al.* report an extinction coefficient of 243 $mM^{-1}cm^{-1}$ for the Soret band (λ_{max} = 422 nm) [Vanderkooi, 1976], determined by lyophilization and direct weighing, in good agreement with this work's values of 239 and 256 $mM^{-1}cm^{-1}$, determined using the Lowry method for protein contents. The α and β peaks occur at 583 and 549 nm in phosphate buffer, pH 7.

Fig. 4.2 also shows the fluorescence emission spectrum. Excitation in any of the absorption bands yields the same emission with maxima at 590 and 640 nm.

There is a slight dependence of the absorption spectrum on pH, (Fig 4.4) reflected in the fluoresecence spectra, but of minimal significance when compared to the marked pH-dependence of the iron-free porphyrin recently observed in the laboratory. [Kornblatt, 1988].

Vanderkooi *et al.* reported a fluorescence lifetime of 3.2 ns for Zn$\underline{c}$ [Vanderkooi,1976] in disagreement with the report of Vos *et al.* of a Zn$\underline{c}$ biphasic decay process with lifetimes

of 0.49 and 1.92 ns [Vos, 1987]. This work (Fig. 4.5) reports that a single exponential describes the Znc fluorescence decay with τ = 1.4 ns.

Further, the Znc shows a triplet absorption maximum at 462 nm with a lifetime of 11 ms and emission maximum at 718 nm with the same lifetime (fig 4.6).

FIGURE 4.2

[A] ABSORPTION SPECTRUM OF Znc - Characteristic of simple square-planar chelates of porhyrins with divalent metal ions, featuring very sharp Soret ($\lambda max \cong$ 422 nm) with α and β bands at 583 and 549 nm [Falk,1964]. ε_{422} = 248 $mM^{-1}cm^{-1}$ in 10 mM phosphate buffer, pH 7.

[B] FLUORESCENCE EMISSION SPECTRUM of Znc - (uncorrected). Emission maxima at 590 and 640 nm, independent of excitation wavelength in 10 mM phosphate buffer, pH 7.

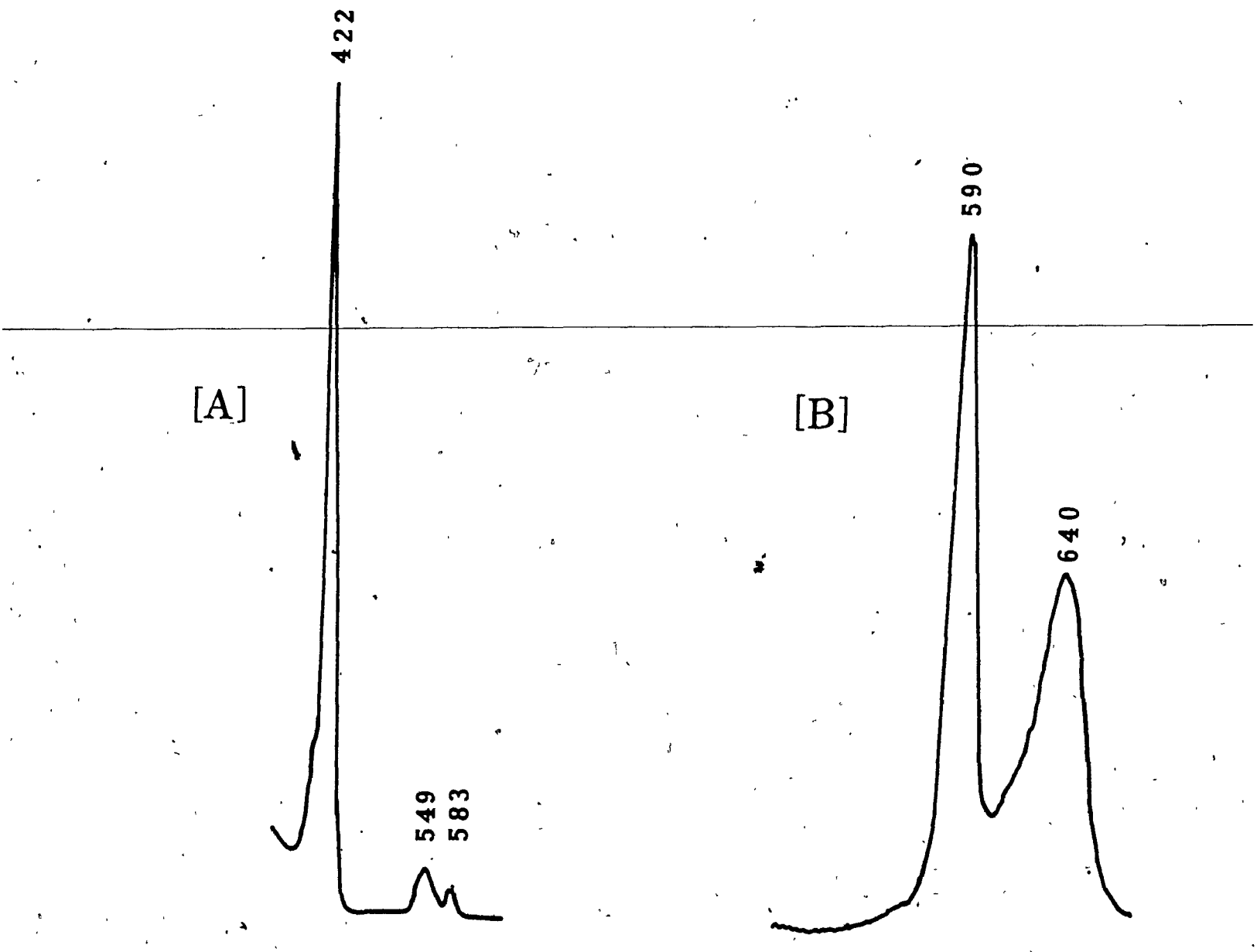
422
549
583
[A]
590
640
[B]

FIGURE 4.3

ABSORPTION SPECTRA OF NATIVE CYTOCHROME c,
PORPHYRIN c and Znc.

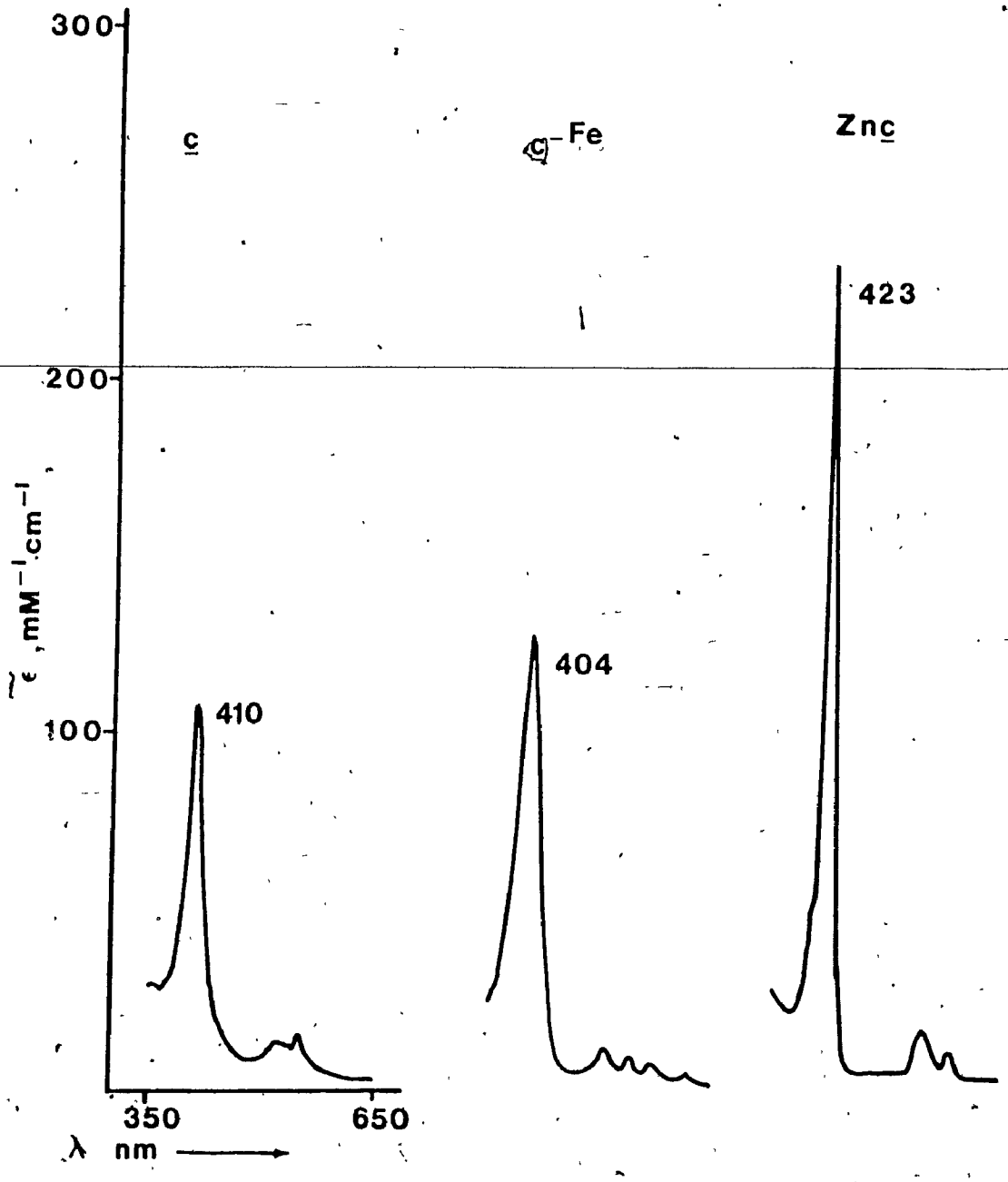
300
200
100
ε, mM⁻¹.cm⁻¹
c
c-Fe
Znc
410
404
423
350
650
λ nm

FIGURE 4.4

pH-DEPENDENCE OF Znc ABSORPTION - Titration of the Soret and α-β bands (not shown) results in increasing absorption with increasing pH. This was observed in EDTA, Bistris and KPi buffer systems. The bottom trace was taken at pH 5.6, the next at pH 6.4 and the last at pH 7.4 . Reversibility was always achieved.

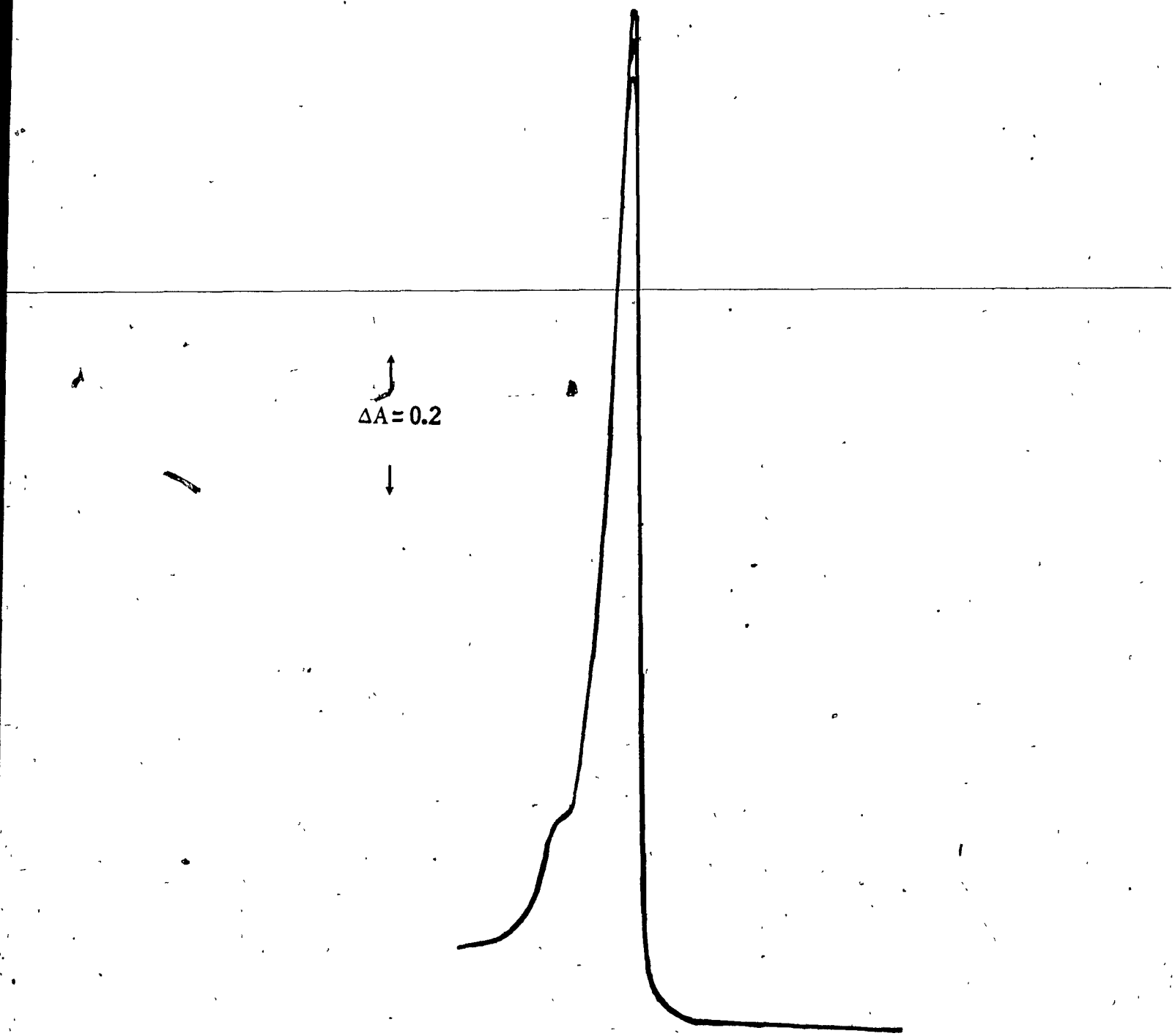
ΔA = 0.2

FIGURE 4.5

FLUORESCENCE DECAY OF Zn_2 - Determined at the Picosecond Centre by the streak-camera method. Lifetime of 640 emission is same as that of 590 emission. Best fit to 256 data points yields a single-exponential decay curve with τ = 1.4 ns in 5 mM phosphate buffer, pH 7.

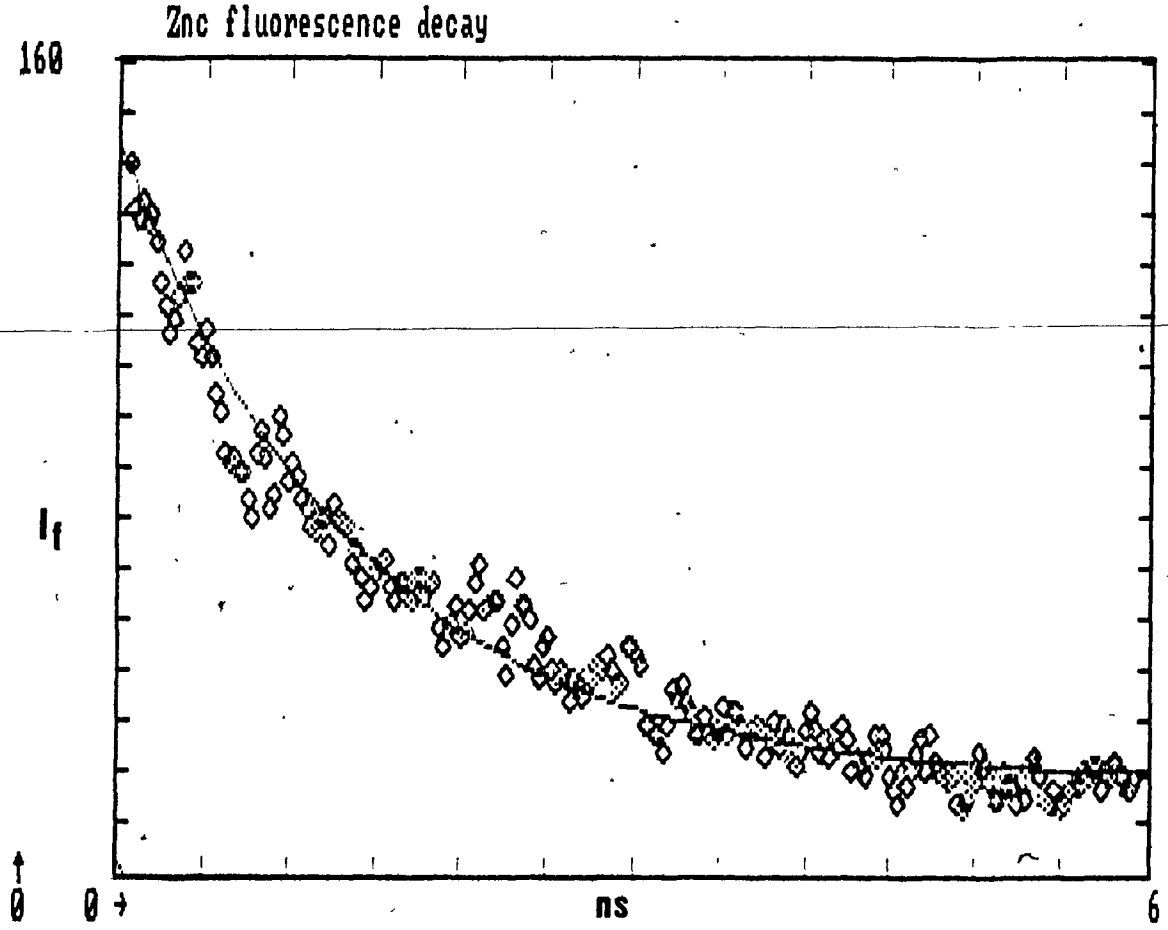
Znc fluorescence decay
160
I_f
0
0
ns
6

FIGURE 4.6

[A] TRIPLET ABSORPTION DECAY of Znc - at 462 nm, τ = 11 ms. Best fit to digitized data. Insert: chart trace.
[B] TRIPLET EMISSION DECAY of Znc - Chart trace at 718 nm. τ = 11 ms.

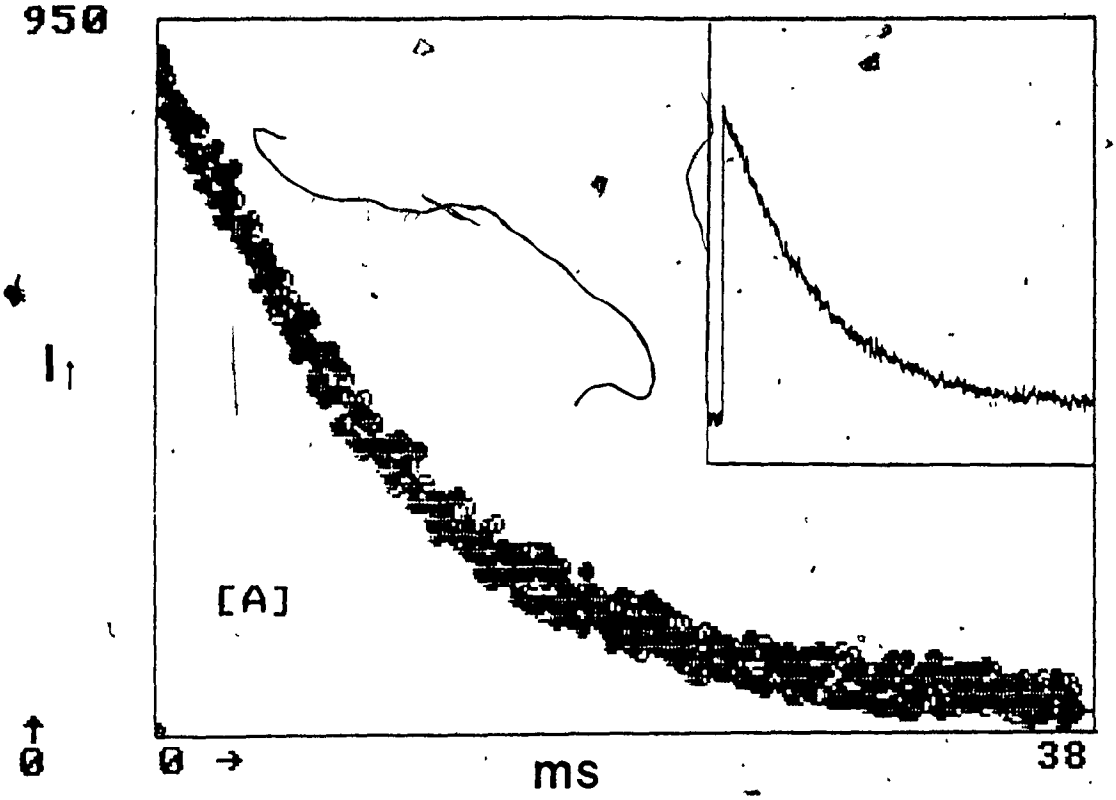
950
I↑
[A]
↑
0
0 →
ms
38

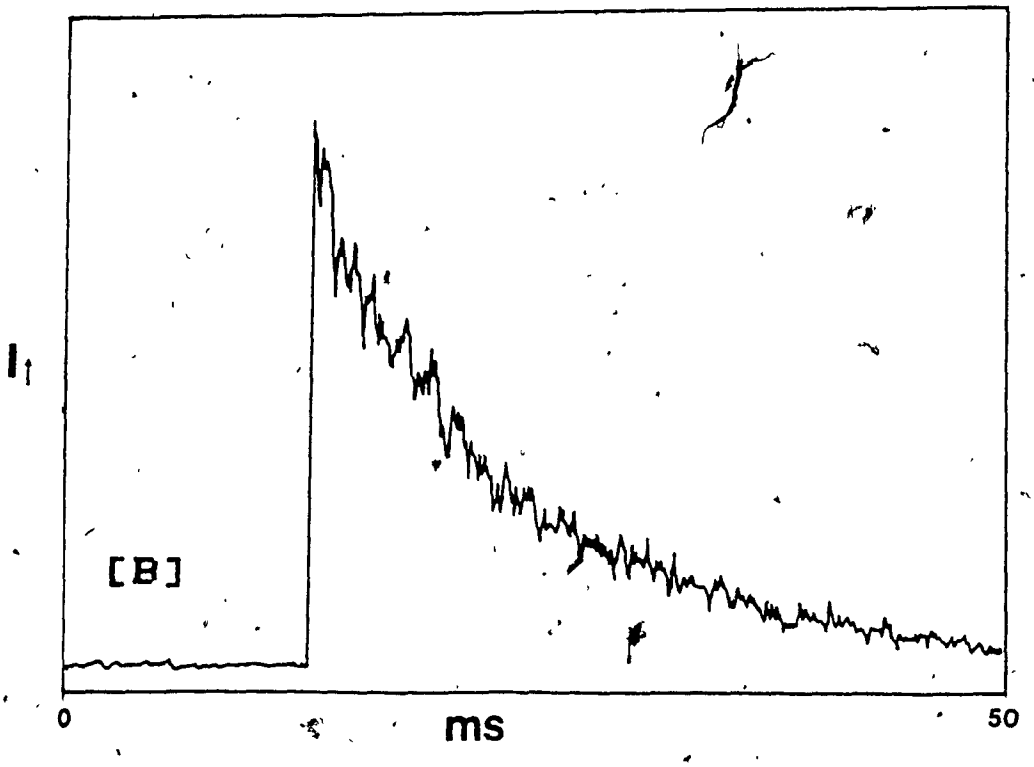
I↑
[B]
0
ms
50

4.3 TIN CYTOCHROME c

4.3.1 SYNTHESIS

Porphyrin c and its metalloderivatives are always handled under minimal light exposure conditions, as they are reported to be susceptible to photodissociation. Such degradation is never observed with c^{-Fe} nor with Znc, but Snc is found to be sensitive to light during synthesis. Tin incorporation is accordingly carried out in total darkness. The procedure is again a modification of that of Vanderkooi [Vanderkooi, 1976].

It is the same as that followed for Znc but $SnCl_2$ is added in 50-fold excess over porphyrin c. After incubation at 40°C, the protein solution is dialyzed against HAc, pH 3, for four hours. A white precipitate is then removed by centrifugation @ 10,000 rpm for 20 minutes. Dialysis against distilled water and 20 mM KPi, pH 5, follows with a last centrifugation yielding a thin film of residual precipitate. The supernatant is concentrated by ultrafiltration (YM 5,000). Unlike Znc, no low molecular weight components are detected.

4.3.2 CHARACTERIZATION

Fig 4.7 shows the absorption spectrum of Snc, with the same sharp features as that of its zinc analog. That the intensity of the α band is close to that of the β band is indicative of chelation stability. The Soret maximum occurs at 409 nm with α and β bands at 574 and 535 nm, respectively in phosphate buffer, pH 7.

Fig 4.7 also shows the fluorescence emission spectrum.As with the zinc species, excitation in any of the absorption bands yields the same emission with maxima at 580 and 636 nm.

In contrast to $\underline{c}^{-Fe}$, and Zn$\underline{c}$, the Sn$\underline{c}$ spectrum remains invariant from pH 5 to 8 (fig.4.8).

Vanderkooi *et al.* report a fluorescence lifetime of 0.8 ns for Sn$\underline{c}$, this work measured a biphasic decay with τ_{fast} = 0.4 ns and τ_{slow} = 1.6 ns (Fig 4.9).

FIGURE 4.7

[A] ABSORPTION SPECTRUM OF Snc - Upon metal chelation, the Soret maximum is shifted from 401 to 410 nm with α and β bands at 574 and 535 nm. ε_{410} = 220 $mM^{-1}cm^{-1}$ in 10 mM phosphate buffer, pH 7.

[B] FLUORESCENCE EMISSION SPECTRUM of Snc - (uncorrected). Emission maxima at 580 nm and 636 nm, independent of excitation wavelength in 10 mM phosphate buffer, pH 7.

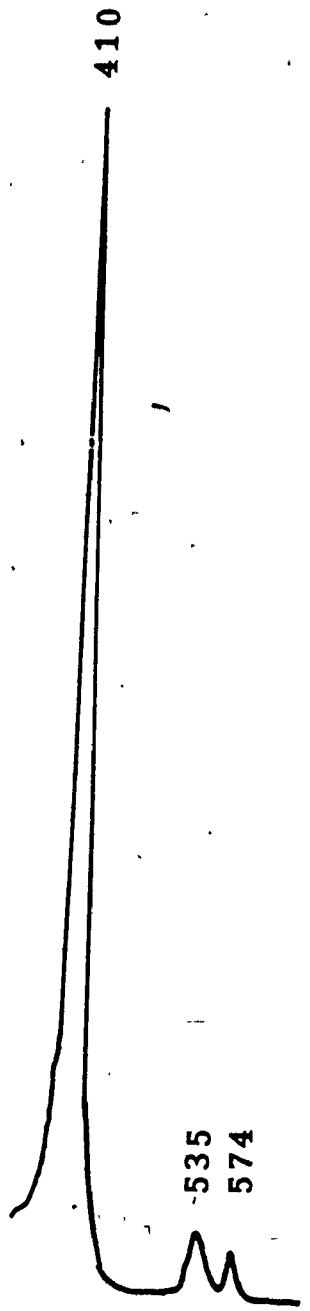
[A]
410
535
574

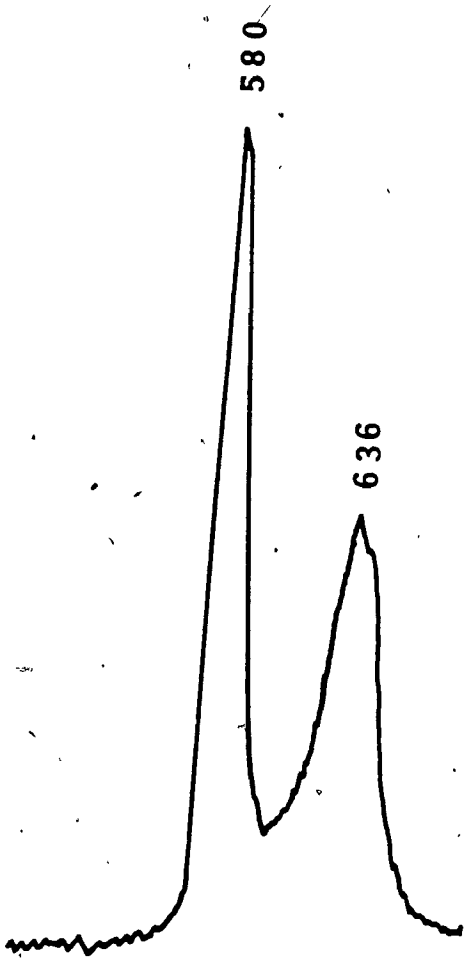
[B]
580
636

FIGURE 4.8

pH-DEPENDENCE OF Snc ABSORPTION - Titration of the Soret and α-β bands (not shown) yields a pH-independent spectrum in the range 5 to 8.

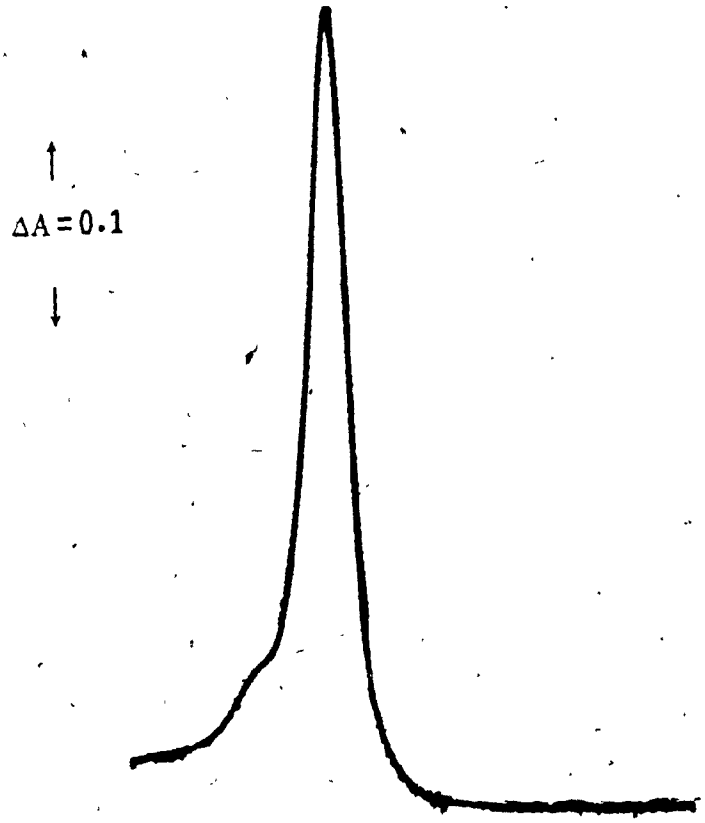
ΔA = 0.1

FIGURE 4.9

FLUORESCENCE DECAY OF Sn_C^{4-} - Determined at the Picosecond Centre by the streak-camera method. Best fit to 256 data points yields a curve which is the sum of two exponentials. One component has τ = 0.4 ns and the other τ = 1.6 ns, in 5 mM phosphate buffer, pH 7.

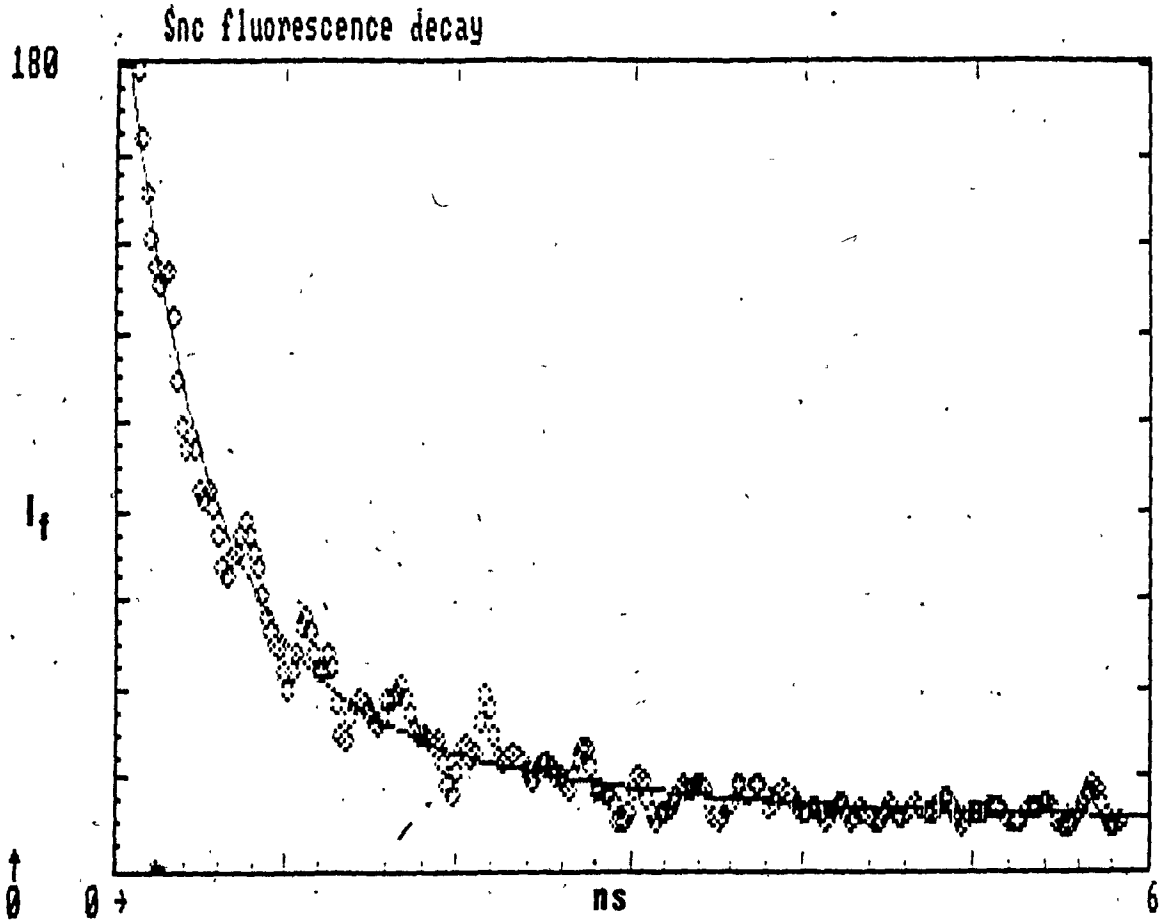
Snc fluorescence decay
180
I_f
0
0
ns
6

4.4 EUROPIUM CYTOCHROME c

4.4.1 SYNTHESIS

After several unsuccessful attempts based on the method used to synthesize the two previous metalloderivatives, the following procedure was found to incorporate Eu^{+3} into cytochrome c's porphyrin: 2 ml of 20 mM KH_2PO_4 are added to 1 ml of 220 μM c^{-Fe} and the pH is lowered to 2.5 with 6N HAc. To this mixture is added 2 ml of 177 μM $EuCl_3$ dissolved in 20 mM phosphate buffer, pH 5. The mixture is then incubated at 40° C for one hour, followed by dialysis against HAc, pH 3 and distilled water. The europium ion however,does not remain coordinated as the pH is increased. Above pH 5, it breaks free from the porphyrin, as seen in the spectrum, which after centrifugation of the sample reverts back to a c^{-Fe} spectrum.

4.4.2 CHARACTERIZATION

When trying to incorporate a rare earth ion into a porphyrin, it is perhaps more accurate to speak of coordination or chelation as the ion's radius (6-coord. Eu^{+3}= 103 pm [Huheey,1983]) prevents a snug fit into the porphyrin's hole. This hole is known to be ideal for first row metals as there is only room for a bond length of 200-205 pm (Fe-N bond length = 218 pm) . Low-spin iron(II) fits well in the hole (radius = 78 pm) while high-spin Fe^{+2} (radius = 95 pm) lies out-of-plane [Perutz, 1970]. Eu(III) is thus expected to lie out-of-plane but its size is not so large as to prevent coordination as first thought. The inability to maintain

chelation at higher pH must therefore depend on chemical rather than stereochemical considerations. This is confirmed by the work of inorganic research groups who are starting to chelate porphyrins to rare earths. That have of course the advantage of being able to work in organic solvents, which allows them to eliminate problems caused by rare earth affinity for coordinating water ligands (trivalent lanthanide ions show strong preference for hard bases; with neutral ligands, the order of preference is O > N > S [Richardson, 1982].

The absorption spectrum shown in Fig 4.11 is close to that of typical inorganic lanthanide pophyrins, which all feature - beside a Soret - three bands in the 500-600 nm range, with the middle band being the most intense [Tsvirko, 1981]. Additional evidence for chelation appears in the presence of the protein peak at 280 nm.

FIGURE 4.10

ABSORPTION SPECTRUM OF EUROPIUM(III) CHLORIDE in distilled water.

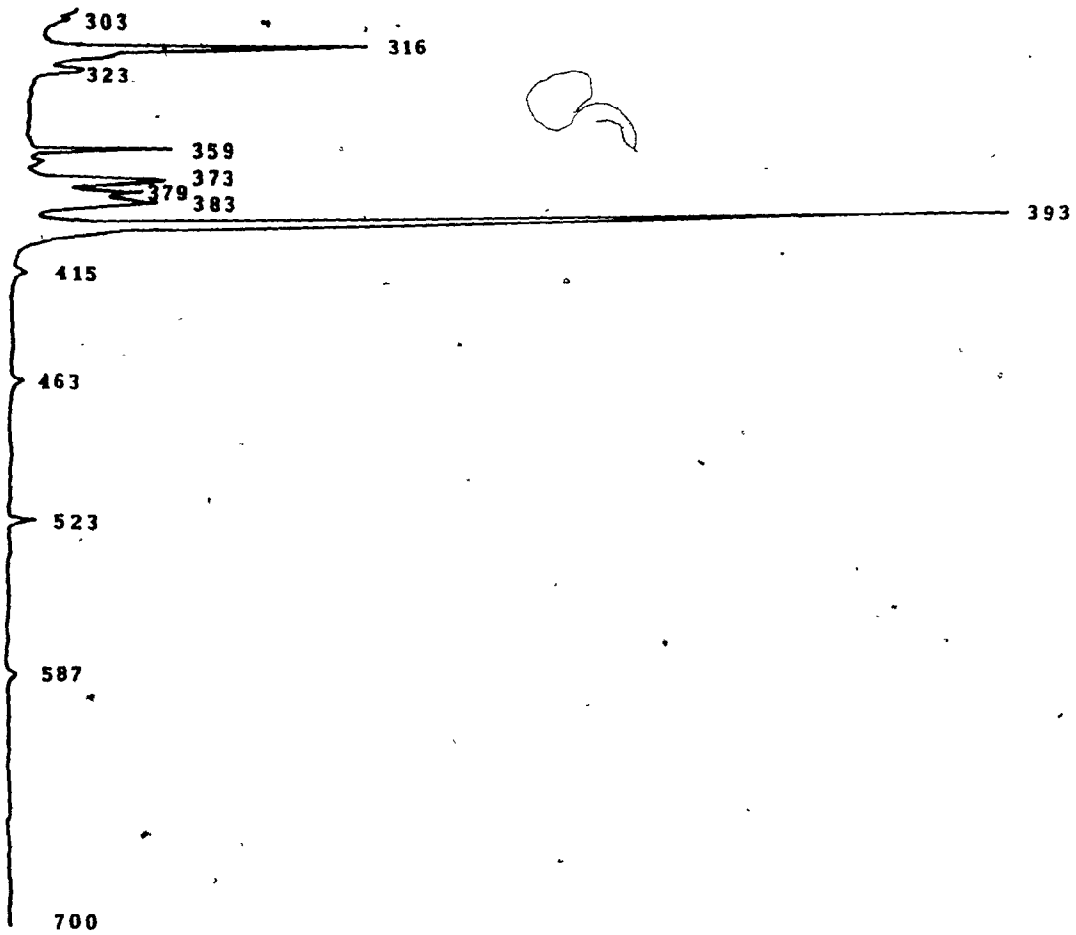
303
316
323
359
373
379
383
393
415
463
523
587
700

FIGURE 4.11

[A] ABSORPTION SPECTRUM OF Euc^{-} in 10 mM EDTA. pH 4.8 . Soret maximum at 403 nm, with bands I to IV at 610, 556, 534 and 501 nm.

[B] FLUORESCENCE EMISSION of Euc^{-} (uncorrected) Emission maxima at 619 and 669 nm, independent of excitation wavelength in 10 mM EDTA, pH 4.8

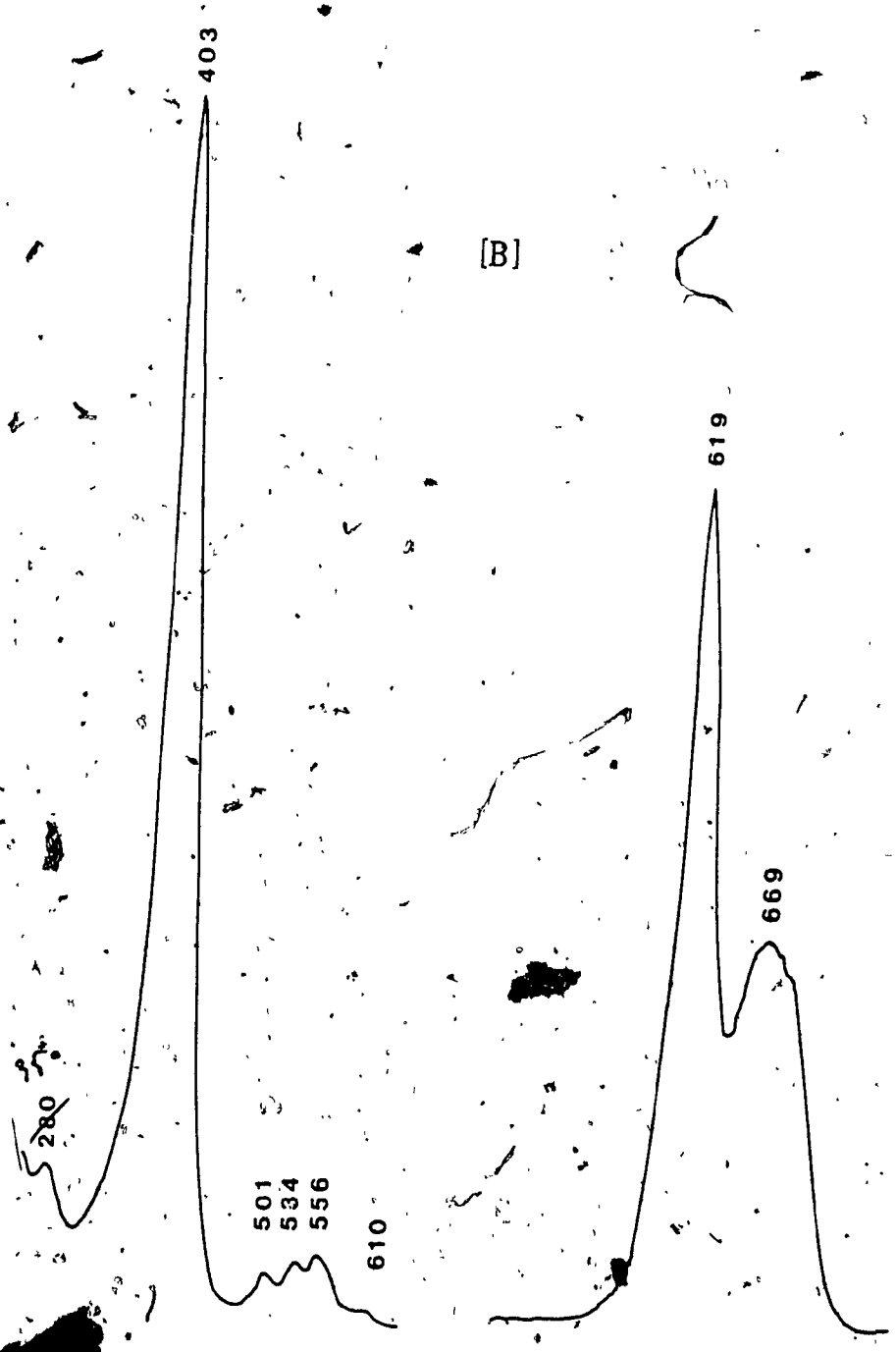
[A]
403
280
501
534
556
610
[B]
619
669

4.5 PURIFICATION OF CYTOCHROME c OXIDASE

Cytochrome c oxidase from beef heart is prepared using the laboratory's standard procedure, adapted from Yonetani's method [Yonetani, 1966]. The procedure is carried out at 4°C.

4.5.1 PARTICULATE PREPARATION

Once obtained from a slaughterhouse, eight hearts are processed so as to remove all connective tissue. They are cubed and ground. This yields ca. 7 kg of muscle. Portions of 1.5 kg are set to wash in a 10 litre-bucket, 1/3 full with crushed ice and brougth to the 7-l mark with distilled water. The mixture is stirred and filtered through two layers of cheese cloth. The filtrate is then washed again in one litre of 0.2 M Na_2HPO_4 diluted to 10 litres with crushed ice and water, stirred every 10 minutes for one hour. The mixture is filtered and washed twice as before with distilled water.

The washed, ground muscle is suspended in cheese cloth, left to drip overnight in the cold room. The next morning, at the crack of dawn, a portion -now weighing ca. 2 kg- is processed further and the others stored at - 20°C. Seven one-litre Waring blenders are connected in series to a rheostat and filled with the following: 150 ml of 0.2 M KPi, pH 7.4; 150 g of crushed ice; 300 g of heart mince. The mixture is homogenized for 7 minutes. The homogenates are collected in the bucket along with enough distilled water to reach the 7-litre mark and centrifuged using a swing-bucket type

centrifuge fitted with one-litre bottle head @ 2,100 rpm (≡ 800 x g) for 20 minutes at 4° C. The supernatant, reddish-brown, cloudy, is collected. The pellet (ca. 1:1 ratio w/supernatant) has a hard part, which is discarded, and a soft, beige component which is stirred into one litre of 0.02 M KPi, pH 7.4, to be rehomogenized for 3 minutes and centrifuged as before. The pellet, this time, is totally discarded and the supernatant added to that of the first centrifugation. This yields some four litres.

The mixture is brought to pH 5.6 using 1 M HAc (ca. 90 ml) and centrifuged for 10 minutes as before.

The supernatant, clear, red, is discarded and the pellet, beige, amounting to some 2 cm (in the one-litre bottles) is dissolved by swirling in distilled water. It is again centrifuged as before. The supernatant, reddish-orange, is discarded and the pellet, hard, beige, is brought to a volume of ca. one litre by addition of 0.1 M KPi, pH 7.4. The pH is adjusted to 7.4 with 3 M NH_4OH (ca. 10 ml).

OXIDASE EXTRACTION

To a particulate preparation of 1090 ml are added 273 ml of 10% cholate which yields 1363 ml of a 2% cholate mixture.(500 ml of 10% neutralized cholic acid are on hand, prepared well in advance by dissolving 50 g of cholic acid into 500 ml of water with the pH adjusted to 7 by addition of 1 N NaOH.).

The mixture is brought to 30% ammonium sulphate saturation by addition of 240 g of solid $(NH_4)_2SO_4$ (i.e 88g per 500 ml).

The solution is left to stand for one hour on ice and centrifuged at 10,000 x g (≡ 10,500 rpm, A-54 head) for 10 minutes. The beige pellet is discarded and the brown, slightly cloudy supernatant is brought to 50% saturation with solid $(NH_4)_2SO_4$ (127 gl^{-1}). The mixture is immediately centrifuged as before. The pellet is resuspended in a total volume of 250 ml of 0.1 M KPi, pH 7.4 in 2% cholate using a hand homogenizer. This solution is brought to 25% saturation by slow addition of 83.2 ml of saturated ammonium sulphate solution and left standing overnight on ice.

AMMONIUM SULPHATE FRACTIONATION

The mixture is centrifuged as before and the hard, beige pellet is discarded. The clear, greenish-brown supernatant is brought to 35% saturation by slow addition of 15.4 ml of saturated ammonium sulphate solution per 100 ml of supernatant and left to stand on ice for 30 minutes. It is centrifuged as before and the slightly cloudy, yellowish supernatant is discarded. The sticky, oily, greenish-brown pellet is resuspended in 80 ml of 0.1M KPi, pH 7.4, 2% cholate and brought to 26% saturation by addition of 34.6 ml of saturated ammonium sulphate solution per 100 ml of solution. Centrifugation as before follows, the thin layer of beige pellet is discarded and the ca. 100 ml of dark green, clear supernatant is brought from 26 to 33% saturation using the following calculation:

$$\text{Final\%} = \frac{[Vi_A \times \%sat_A] + [V_S \times \%sat_S]}{Vi_A + V_S} \qquad (4.1)$$

where Vi_A = volume of supernatant

$\%sat_A$ = percent saturation of supernatant

V_S = volume of saturated ammonium sulphate required

$\%sat_S$ = percent saturation of saturated ammonium sulphate = 100%

The equation is solved for V_S, which is the volume of saturated ammonium sulphate solutionto be added to the supernatant.

The mixture is centrifuged as before, the supernatant, yellowish, is discarded, the oily oxidase pellet is taken up in the following buffer: 1% tween, 10 mM Tris, 10 mM Na_2EDTA, 100 mM KCl, 1 mM NaF, pH 7.2. The solution is brought to 31 % saturation (31 ml of saturated ammonium sulphate per 70 ml of supernatant) and centrifuged as before. The supernatant is discarded and the pellet again resuspended in the above buffer. The procedure yields an oxidase which satisfies the following purity criteria:

- complete removal of cytochromes b and c_1 bands at 560 and 552 nm;
- removal of the oxidase impurity band at 422 nm in the reduced spectrum;
- A ratio of $A_{445(red)}/A_{422(ox)}$ = 1.25 or more;
- A ratio of $A_{280(ox)}/A_{445(red)}$ = 2.5 or less.

Fig 4.12 shows the spectrum of the oxidase routinely obtained with this purification procedure.

This ca. 250 μM extract can be stored at - 10° C until

required. When thawed, ca. 2 ml are diluted to 4 ml with the 100 mM KCL above buffer and chromatographed on a CL-6B gel filtration column to remove the extraction cholate and high molecular weight aggregates.

FIGURE 4.12

ABSORPTION SPECTRUM OF CYTOCHROME c OXIDASE - 7.6 μM, prepared as described in text. Full trace: oxidized; dashed trace: reduced with sodium dithionite. $\Delta\varepsilon_{605(red-ox)}$ = 11 $mM^{-1}cm^{-1}$; $\varepsilon_{422(ox)}$ = 70 $mM^{-1}cm^{-1}$ [Kornblatt, 1986]. Insert: 45 μM haem a, from 580 to 900 nm.

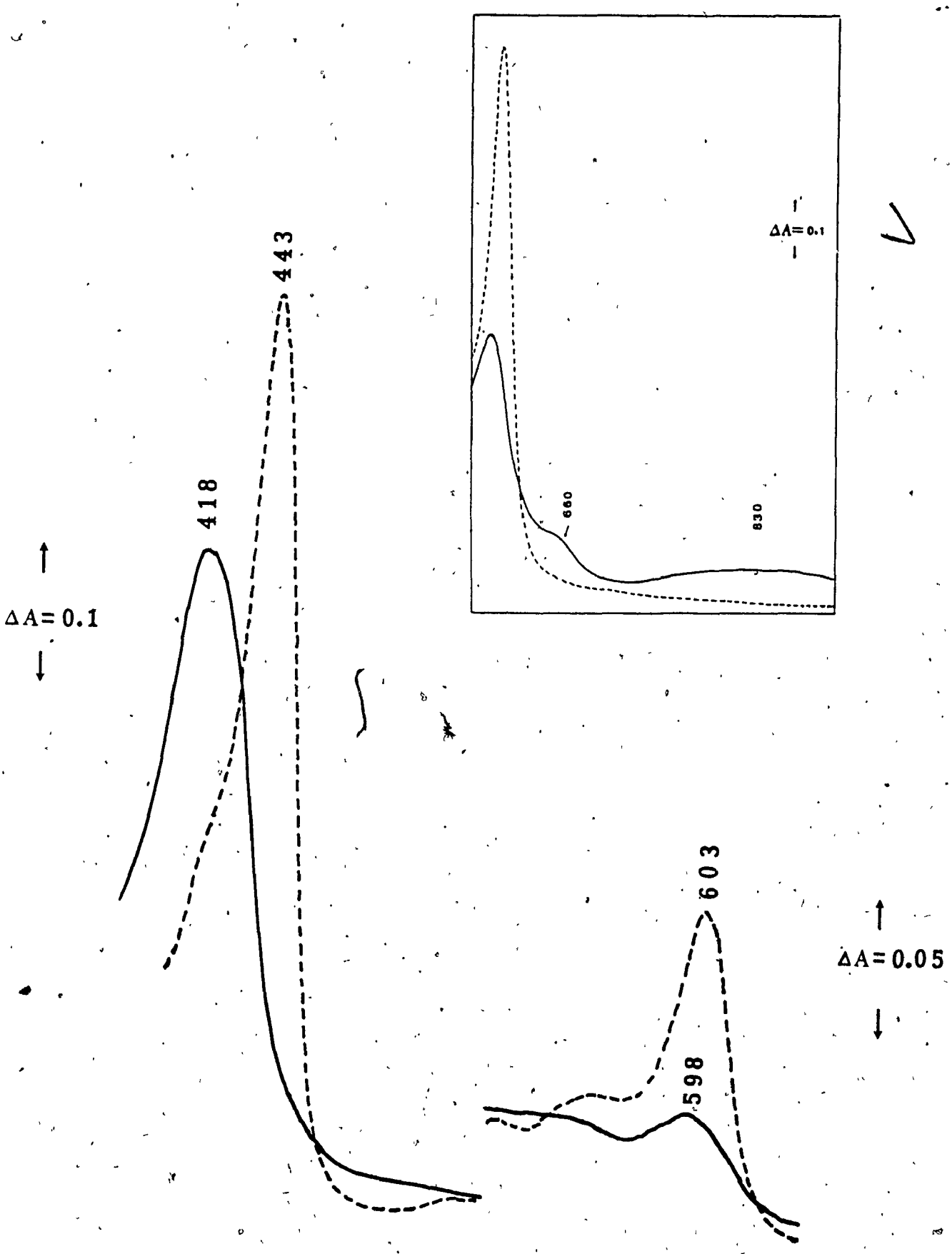
ΔA= 0.1
418
443
ΔA= 0.1
660
830
603
598
ΔA= 0.05

4.6 COMPLEXES OF CYTOCHROME c OXIDASE AND METALLODERIVATIVES

Vanderkooi *et al.* first made use of the fluorescence properties of these derivatives in the context of oxidase binding studies. As shown in Fig 4.14, there is good overlap between the emission of Snc and Znc with the absorption spectrum of the oxidase. Complex formation is thus expected to result in Förster-type energy transfer from the donor (the metalloderivative) to the acceptor (the oxidase) [Vanderkooi, 1977]. These authors reported a 20% quenching of Snc fluorescence by the oxidase and 30% quenching of Znc fluorescence by the same. This is expected in view of the better emission/absorption overlap in the Znc case. What motivated this part of the work was to determine the stoichiometry of binding of the oxidase and the cytochrome c analogs, which Vanderkooi *et al.* had not reported on .To do this, two methods were used.

4.6.1 FLUORESCENCE TITRATION

In a typical titration, 20 ml of stock 0.9 μM Znc or Snc is prepared and 2 ml-aliquots are introduced into 10 test tubes. The oxidase (40 μM haem aa_3) is added in 10 or 20 μl-aliquots along with buffer (1 mM KPi, pH 7, 0.5% Tween 80) so that all tubes have a constant final volume (2.65 ml) and metalloderivative concentration (0.7 μM).Corrections for inner filtering are made using:

$$F_c = F \text{ antilog } [(A_{ex} + A_{em})/2 \qquad (4.2)$$

where F_c is the corrected fluorescence intensity, F is the

measured intensity, A_{ex} is the absorbance of the sample at the excitation wavelength and A_{em} the absorbance of the sample at the emission wavelength [Hill, 1986]. An additional correction is made to control for the addition of the absorbing species. Following Alleyne *et al.*, [Alleyne,1987] the same titration is repeated in high ionic strength buffer (300mM overall). The slight quenching observed and which can not be due to complexation is also corrected for. The fluorescence of the Zn$\underline{c}$/Sn$\underline{c}$ sample -without oxidase is set at 90%- and the fluorescence of each tube is read upon addition of the oxidase aliquot. For Zn$\underline{c}$, the excitation wavelength is set at 422 or 549 nm with emission monitored at 590 or 640 nm. Sn$\underline{c}$ is excited either at 409 or 535 nm and the emission read at 580 or 636 nm.

Figs 4.13 and 4.14 show that the stoichiometry of binding for both metallocytochrome $\underline{c}$'s is one per functional unit of oxidase (aa_3).

4.6.2 GEL FILTRATION

In this experiment, mixtures of the oxidase and the cytochrome $\underline{c}$ derivatives are prepared as follows:

A thawed oxidase extract is first loaded on a CL-6B gel column for final purification. The main band eluate (ca. 40-50 μM haem aa_3) is dialyzed against 1 mM KPi, 0.5% Tween 80, pH 7 to lower the ionic strength. Typically, 2 ml of 36 μM aa_3 are added to 1 ml of 200 μM Zn$\underline{c}$ or Sn$\underline{c}$ in the same buffer for final concentrations of 24 μM oxidase in 67 μM

derivative. The sample is loaded onto a Sephadex G-75 gel filtration column (46 Ø x 0.8 cm) equilibrated in the same buffer and eluted under minimal light exposure conditions at 4° C at a flow rate of 6 mlh^{-1}. The elution profile always shows sharp separation of the complex and the excess derivative. The fluorescence of the fractions is monitored at the appropriate wavelengths as well as the Soret absorption. The stoichiometry of binding is determined by anaerobic reduction of a complex fraction. A sodium dithionite solution is prepared and degassed in a Thunberg tube and a gas-tight syringe is used to transfer the reducing agent to capped cuvettes containing the degassed fraction. Oxidized and reduced spectra are recorded. The concentration of oxidase is determined using ε_{442}= 200 $cm^{-1}mM^{-1}$, ε_{423}= 94 $cm^{-1}mM^{-1}$ and ε_{410}= 63 $cm^{-1}mM^{-1}$ (haem aa_3 basis, reduced) and that of the metallocytochrome c using ε_{423}= 248 $cm^{-1}mM^{-1}$ for Znc and ε_{410}= 220 $cm^{-1}mM^{-1}$ for Snc.

FIGURE 4.13

QUENCHING OF Znc FLUORESCENCE BY CYTOCHROME c OXIDASE. [A] At low and high ionic strength (μ); [B] due to complexation only.

A:

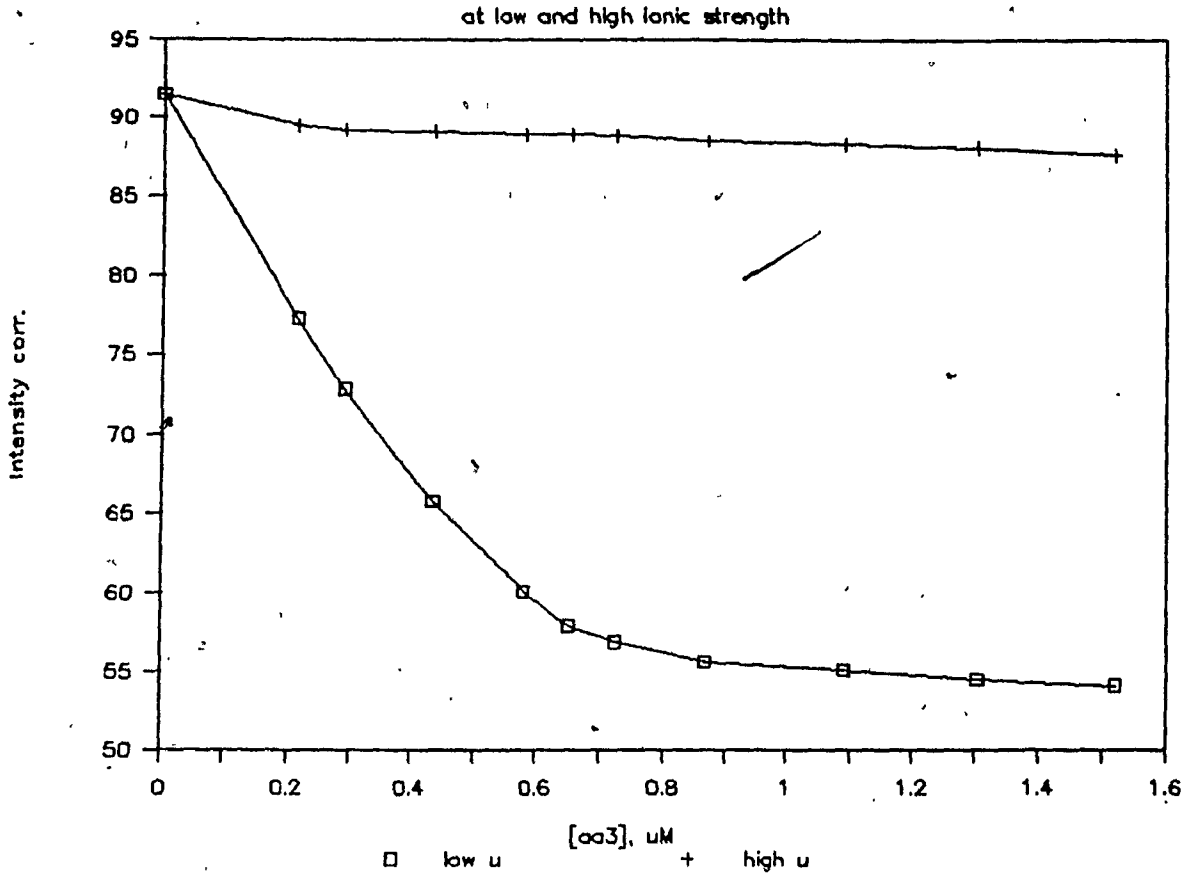
at low and high ionic strength
Intensity corr.
95
90
85
80
75
70
65
60
55
50
0
0.2
0.4
0.6
0.8
1
1.2
1.4
1.6
[oa3], uM
low u
high u

B:

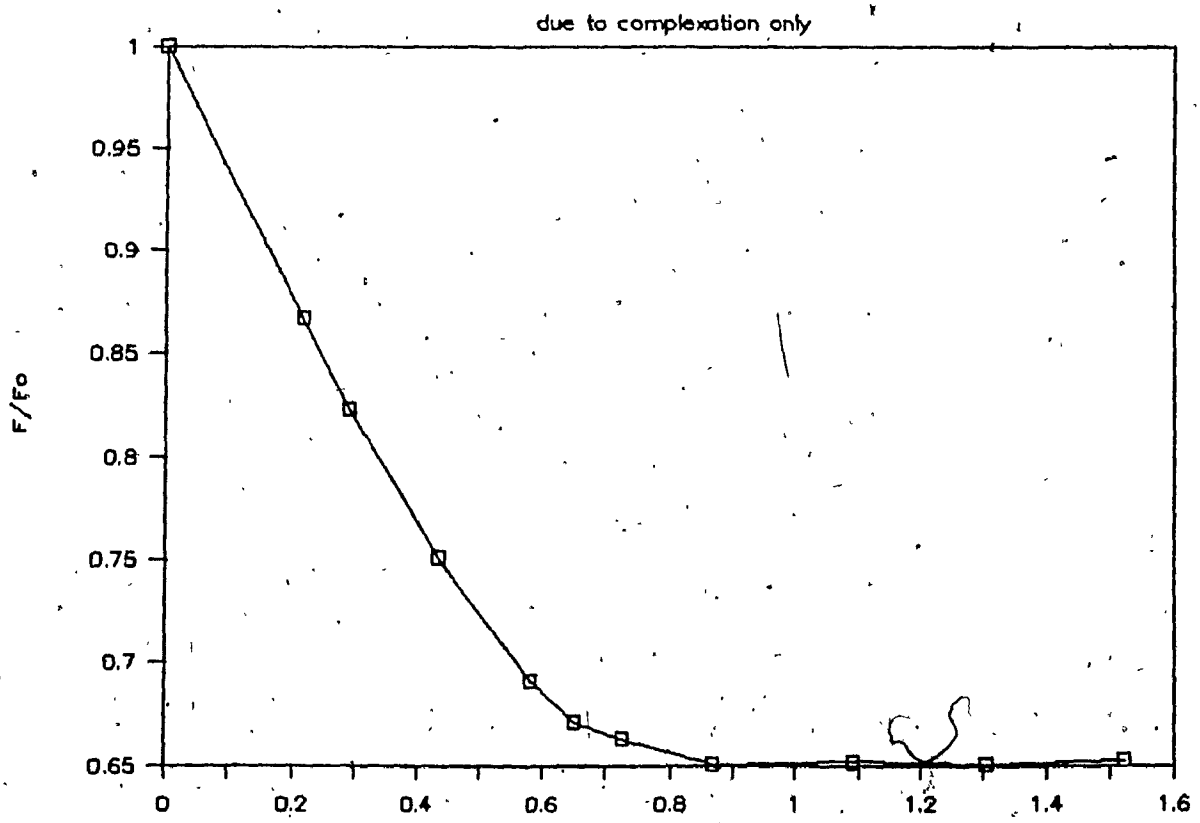
due to complexation only
F/Fo
1
0.95
0.9
0.85
0.8
0.75
0.7
0.65
0
0.2
0.4
0.6
0.8
1
1.2
1.4
1.6

FIGURE 4.14

QUENCHING OF Sn$\underline{c}$ FLUORESCENCE BY CYTOCHROME $\underline{c}$ OXIDASE DUE TO COMPLEXATION.

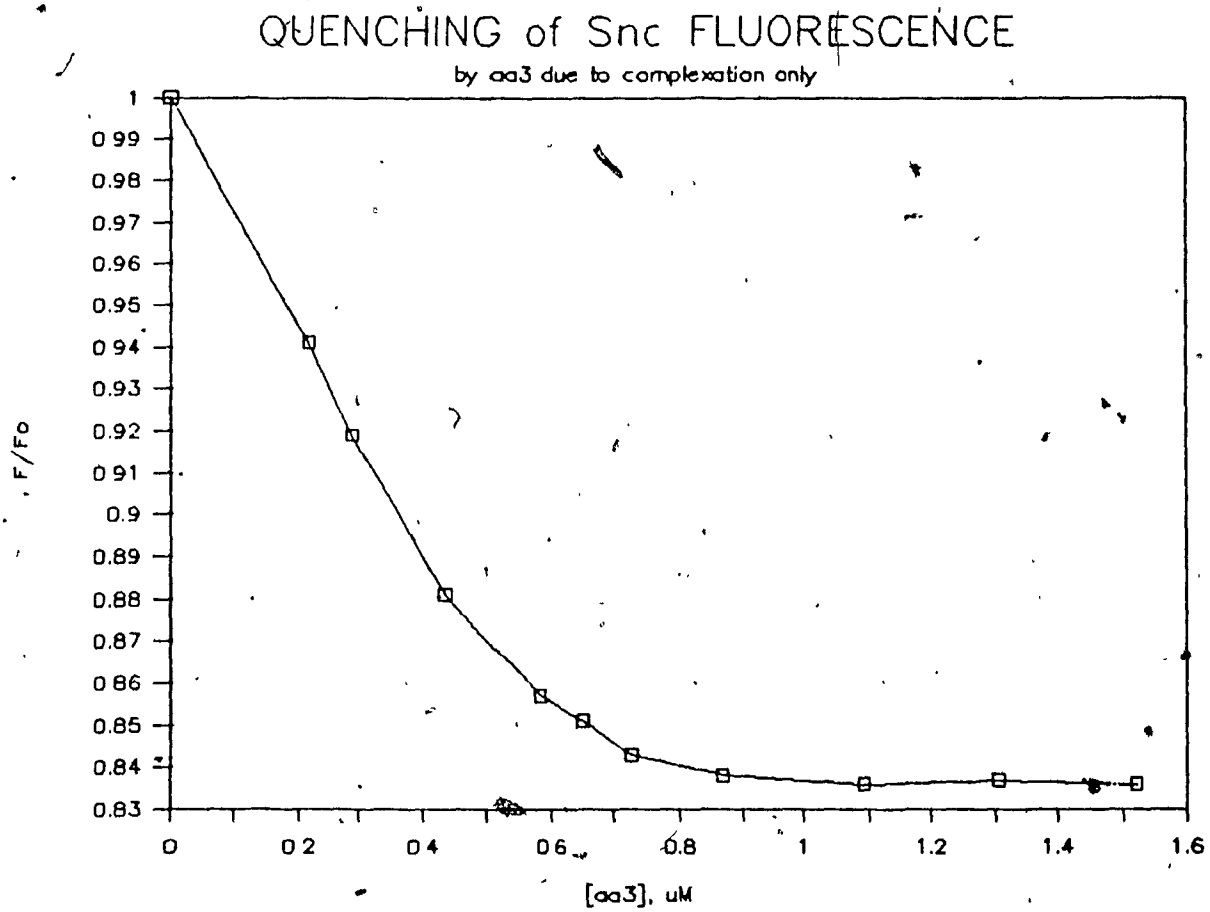
QUENCHING of Snc FLUORESCENCE
by aa3 due to complexation only
F/Fo
1
0.99
0.98
0.97
0.96
0.95
0.94
0.93
0.92
0.91
0.9
0.89
0.88
0.87
0.86
0.85
0.84
0.83
0
0.2
0.4
0.6
0.8
1
1.2
1.4
1.6
[aa3], uM

FIGURE 4.15

ABSORPTION SPECTRUM OF THE Znc:OXIDASE COMPLEX - Full line: oxidized: dashed line: reduced, in 1 mM KPi, pH 7.

Concentrations of Znc ([Znc]) and oxidase ($[aa_3]$) determined using Beer's law after reduction:

$$A_{423} = A_{Znc} + A_{aa3} = \varepsilon_{Znc,423}[Znc] + \varepsilon_{aa3,423}[aa_3]$$

$$A_{442} = A_{Znc} + A_{aa3} = \varepsilon_{Znc,442}[Znc] + \varepsilon_{aa3,442}[aa_3]$$

or:

$$A_{423} = 0.77 = 248\ cm^{-1}mM^{-1}[Znc] + 94\ cm^{-1}mM^{-1}[aa_3]$$

$$A_{442} = 0.41 = 1\ cm^{-1}mM^{-1}[Znc] + 200\ cm^{-1}mM^{-1}[aa_3]$$

Solving the set of simultaneous equations yields: [Znc] = 2.3 μM and $[aa_3]$ = 2.1 μM.

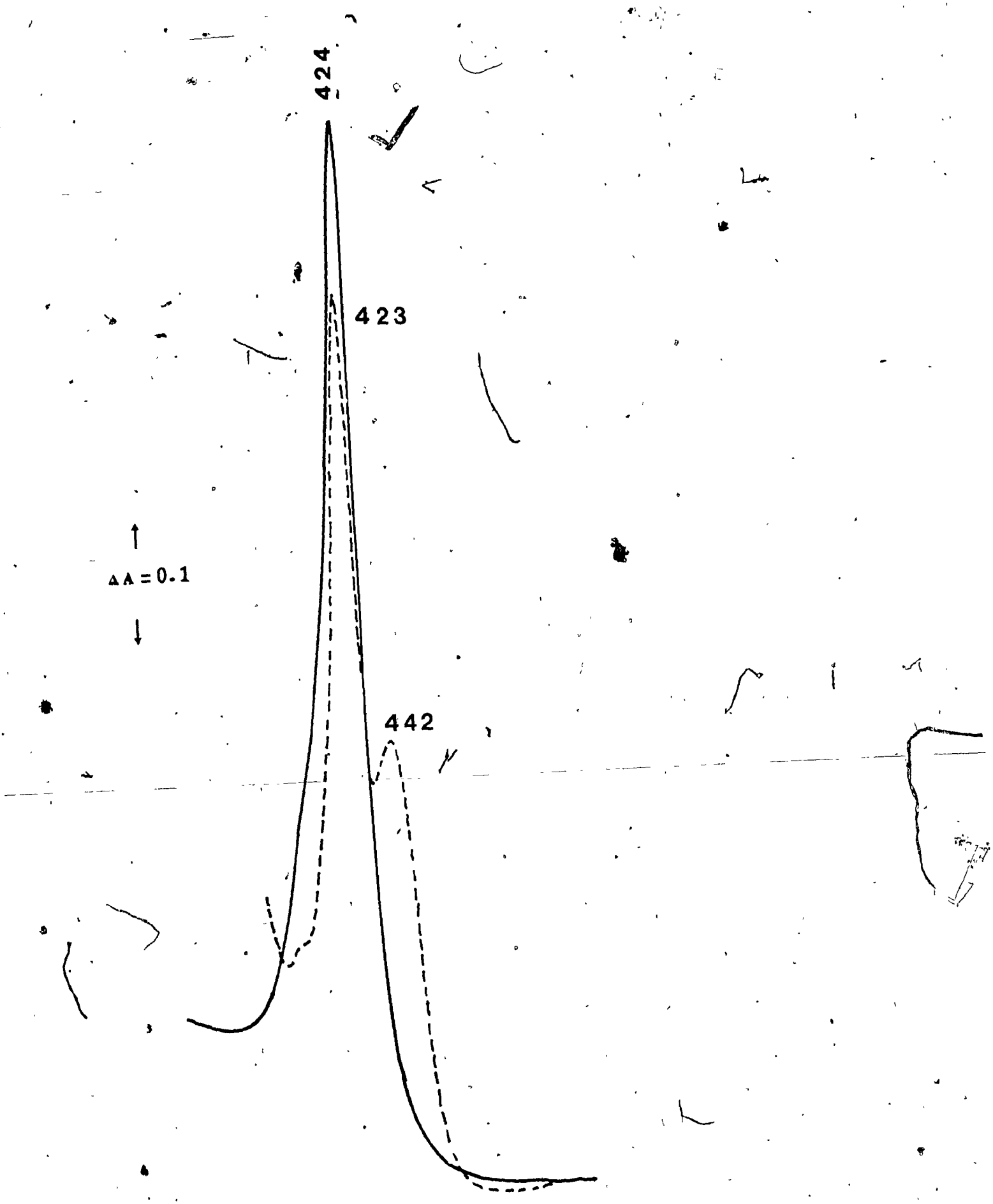
424
423
442
ΔA = 0.1

FIGURE 4.16

ABSORPTION SPECTRUM OF THE Snc:OXIDASE COMPLEX - eluted from Sephadex G-75 in 1 mM KPi, 0.5% Tween, pH 7. Insert: Upon reduction, the 420 nm shoulder in the oxidized spectrum grows into the reduced 442 nm band. The stoichiometry of binding is one Snc per haem aa_3.

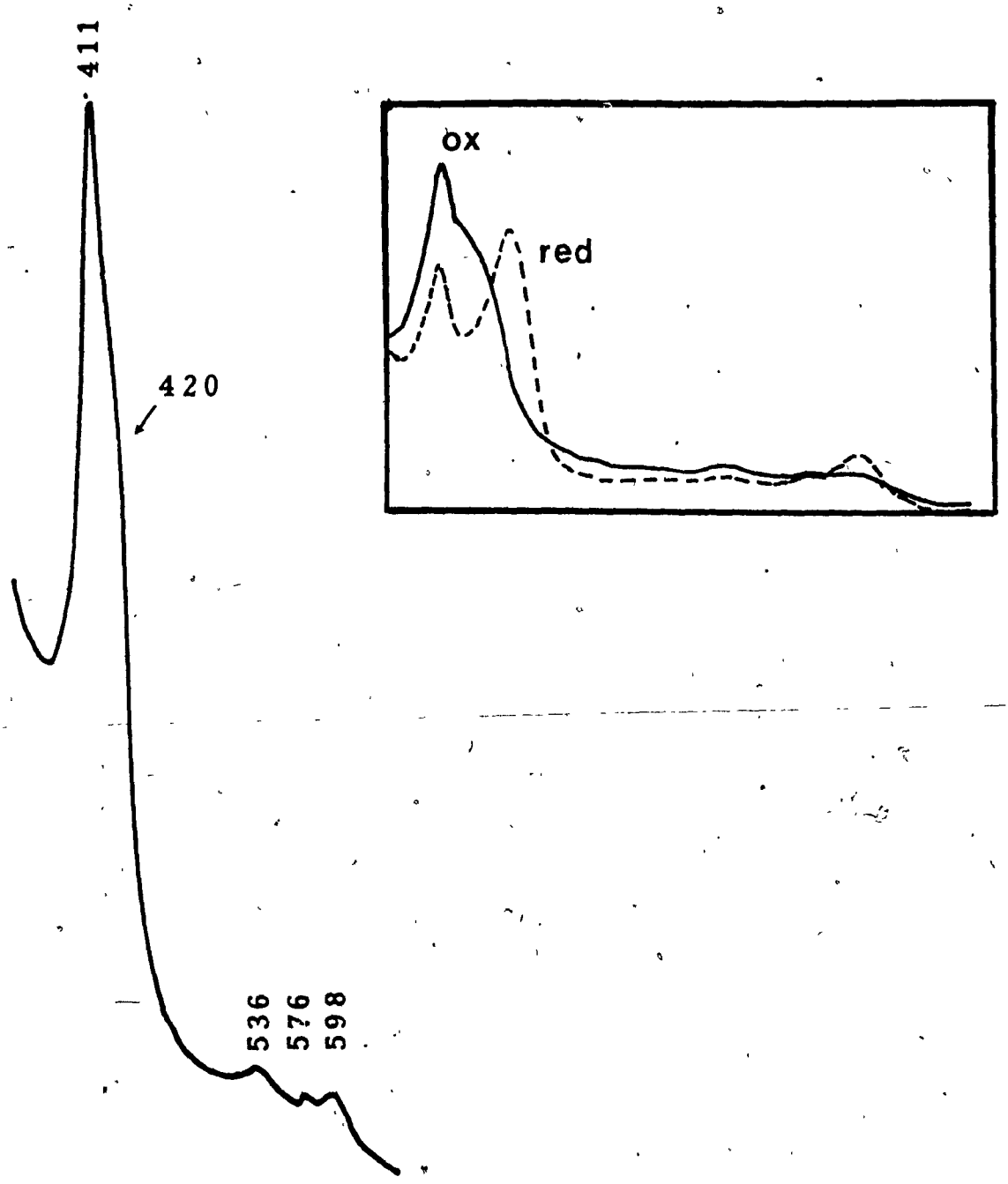
411
420
536
576
598
ox
red

REFERENCES

Alleyne, T. A. and M. T. Wilson, Biochem J., 247, 475 (1987).

Falk, J.E., Porphyrins and Metalloporphyrins; Elsevier, Amsterdam, 1964.

Fisher, W.R.; Taniuchi, H.and C. B. Anfinsen, J. Biol. Chem., 248, 3188 (1973).

Hill, B. C.; Horowitz, P. M. and N. C. Robinson, Biochem., 25, 2287 (1986).

Huheey, J. E., Inorganic Chemistry, Harper & Row, Cambridge, 1983.

Kornblatt, J. A. and M. Laberge, Eur. J. Biochem., 1988, in press.

Kornblatt, J. A. and H. A. Luu, Eur.J. Biochem., 159, 407 (1986).

Kornblatt, J. A.; Bon Hoa, G. H. and A. M. English, Biochem., 23, 5906 (1984).

Perutz, M. F., Nature, 228, 726 (1970).

Richardson, F.S., Chem. Rev., 82, 541 (1982).

Robinson, A. B. and M. D. Kamen, Structure and Function of Cytochromes; Okonuk, K. et al., Eds; Tokyo, 1968

Tsvirko, M. P.; Solovev, K. N.; Stelmakh, G. F.; Pyatosin, V. E. and T. F. Kachura, Opt. Spektrossk., 50, 555 (1981).

Vanderkooi, J. M.; Landesberg, R.; Hayden, G. W.and C. S. Owen, Eur. J. Biochem., 81, 339 (1977).

Vanderkooi, J. M.; Adar, F. and M. Erecinska, Eur. J. Biochem., 64, 381 (1976).

Vos, K.; Laane, C.; Weijers, S. R.; Van Hoek, A.; Veeger, C. and A. J. Visser, Eur. J. Biochem., 169, 259 (1987).

Yonetani, T., Biochem. Prep., 11, 14 (1966).

5. QUENCHING OF TRIPLET ZNC BY CYTOCHROME C OXIDASE

5.1 EXPERIMENTAL STRATEGY

As soon as Znc was available in sufficient quantities, an attempt was made to photoinduce electron transfer to the oxidase.Quenching of the Znc transient triplet absorption was duly observed in the presence of the oxidase and the following approach was used to answer pertinent questions:

1. Determination of the ^{3}Znc absorption and emission spectra in the visible range;
2. Monitor decay at several wavelengths to ensure that only one transient species is formed;
3. Select appropriate wavelengths to observe electron transfer products; these were 586 nm and 602 nm to monitor haem a_3 and a reduction as well as a a wavelength where the oxidized and reduced spectra of the oxidase are isosbectic (563 nm) so as to monitor the Znc quenching rate unperturbed by the growth of a reduced species;
4. Perform the quenching experiment using the fully reduced enzyme -which can not be an electron acceptor;
5. Determine the effect of adding a species which can accept neither energy nor electrons from ^{3}Znc, such as native cytochrome c (II).

FIGURE 5.1

EXPERIMENTAL SET-UP FOR TRANSIENT ABSORPTION MEASUREMENTS - A Phase-R dye laser (1) is used to flash a Znc sample in the cell compartment (2). A tungsten-halogen lamp (3) beam monitors monitors the transient absorption changes. It is directed through a pin-hole and collimated through the sample. The emerging beam is focused to a monochromator (5) placed in front of the photomultiplier tube (6). A power supply unit (7) provides the required voltage to the PMT; the signal is sent to an oscilloscope (8).

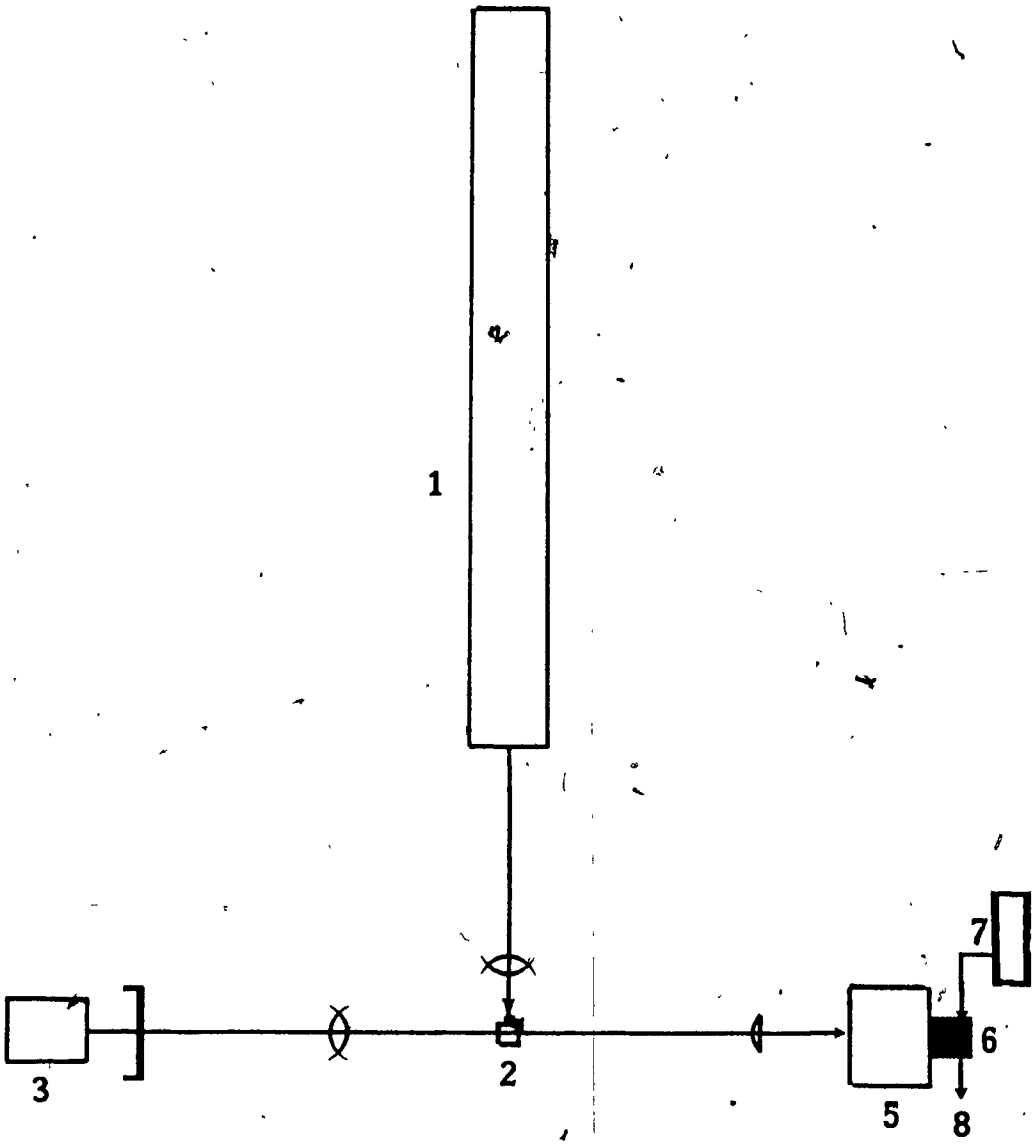
1
2
3
5
6
7
8

5.2 EXPERIMENTAL

5.2.1 METHODS

To avoid the complex kinetics of bimolecular reactions, the experiments were at all times performed on the tight, 1:1 complex (K_A = 7 x 10^6 M^{-1} [Wilson, 1987]), prepared as described in section 4.6.2. Alternatively, the complex was also prepared by mixing appropriate amounts of Znc and oxidase. The samples were placed in capped cells and degassed under purified nitrogen for 30 minutes before flashing. For the reduced oxidase experiment, stoichiometric amounts of degassed sodium dithionite were added to the sample cell with a gas-tight Hamilton syringe. All experiments were performed at room temperature and spectra were recorded before and after flashing on a Cary spectrophotometer.

5.2.2 INSTRUMENTATION

A Phase R DL-2100C dye laser supplying (@ 15 kV) ca. 0.8 J pulses of < 200 μsec, was used to excite the samples.The dye was rhodamine 6G (#M94) dissolved in spectral grade methanol (5 x 10^{-5} M). The experimental set-up is shown in Fig 5.1 .

The maximum lasing wavelength is at 578 nm which allows for pumping of the triplet via Znc's 580 nm band.

A Philips 15 V-150 W # 6423; EFR A1/232 tungsten-halogen lamp was used to monitor absorption changes. The signal photomultiplier was a red-sensitive Hamamatsu R-928 (detection range: 185-930 nm). The signal was fed through a

5.1 kΩ termination to an oscilloscope and traces were recorded on a strip chart recorder. For absorption measurements, 700 V were applied to the PMT and 800 V were applied for emission.

5.3 DATA TREATMENT

The recorder traces were enlarged and the data was digitized by hand. LOTUS 1-2-3 was used as a spreadsheet and unformatted data files were created. F-CURVE software (© Noggle, 1985) was used for curve-fitting on an IBM XT with MS-DOS 3.2. The curve-fitting program uses the simplex algorithm.

A simplex is a triangle that has one more vertex than the dimension of the space in which it exists (Fig. 5.2). If there are NP parameters, the number of vertices of the simplex NV becomes NV = NP + 1. The initial location of the vertices was determined by estimating the parameters from the strip chart traces which yielded the maximum and minimum signal intensities as well as rough lifetimes from the widths at half-maximum of the decays. Then, for each vertex, the program calculates the best response and worst response. For two parameters, there are three vertices that can be ranked as best (B), second best (S) or worst (W). The centroid of all points but the worst is calculated as a sum of coordinates of the points. The worst point is then reflected through the centroid to yield a reflected point and a reflected value is calculated for each coordinate. The

FIGURE 5.2

THE SIMPLEX - For two parameters, there are three vertices that are ranked as to response as best (B), second best (S) and worst (W).

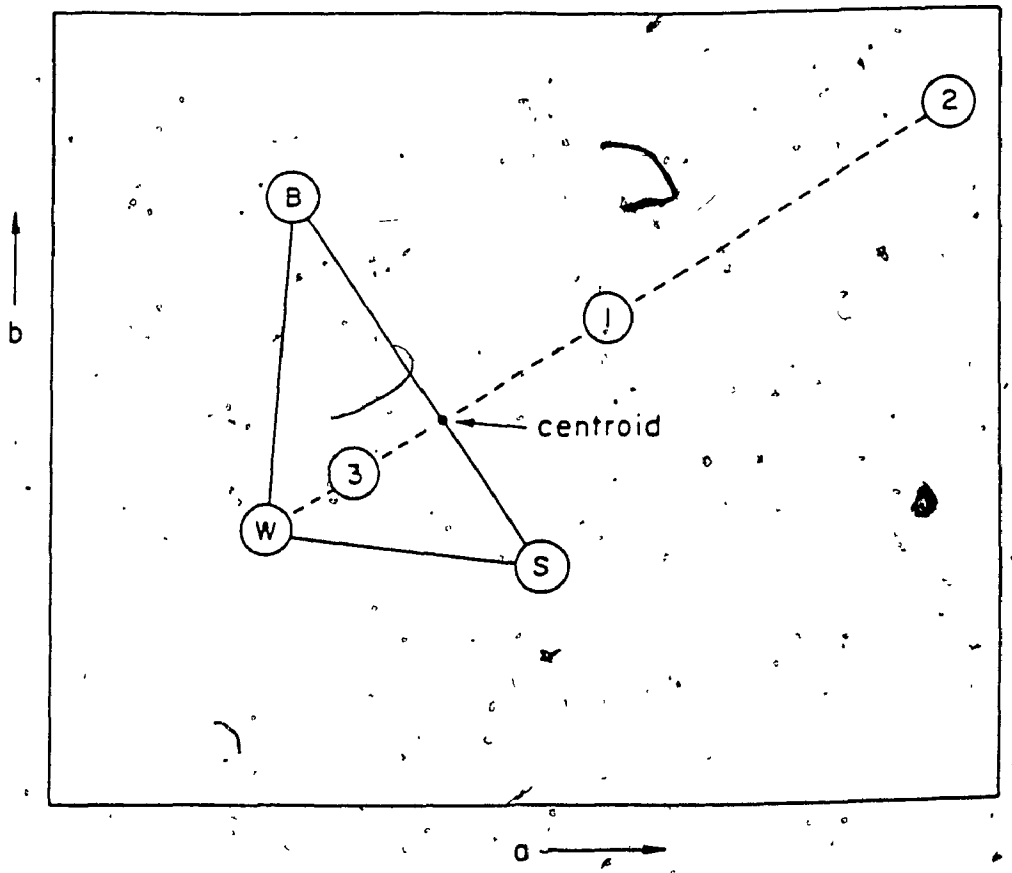
B
2
1
centroid
3
W
S
b
a

response is then calculated at the reflected point. If the reflected point is better than the best then the simplex is expanded. The response at the new point is measured. If this is better than the reflected point, the expanded point is accepted in place of the worst point and a new simplex is created. The procedure is repeated until the best fit is obtained [Noggle, 1985].

The method of weighted least-squares was also used on linearized data, as outlined by Demas [Demas, 1983].

5.4 RESULTS

5.4.1 ^{3}ZnC/ZnC DIFFERENCE SPECTRUM

Fig 5.3 shows the ^{3}ZnC/ZnC difference spectrum obtained by flashing a ZnC sample at 10 nm-intervals. Five flashes were observed at each wavelength and the average voltage change recorded. Conversion to absorbance units was obtained using:

$$I = I_o \times 10^{-\varepsilon bc} \qquad (5.1)$$

$$A = -\log T \qquad (5.2)$$

$$A = \log I_o/I \qquad (5.3)$$

where A is the absorbance, T the transmittance, I_o is the incident light, equal to 100% transmittance and I is the transmitted light. At given applied voltages, care was taken to verify that the singlet spectra thus obtained matched those obtained from a commercial spectrophotometer. Transient triplet difference spectra were then obtained at 65, 70 and 75 % conversion. In the course of recording these spectra,

the lifetime of ^{3}Znc remained invariant at all wavelengths. The triplet maximum occurs at 460 nm and accurate wavelength monitoring places it at 462 nm. A shoulder appears at ca. 525 nm.

Isosbectics occur at 432, 570 and from 590 to 640 nm.

TABLE 5.1: Experimental Measurements recording the ^{3}Znc/Znc Difference Spectrum shown in Fig 5.3

λ, nm	Io(mV)	I(mV)	A,gs	ΔV(mV)	A,triplet	ΔA
400	90	40	0.35	- 10	0.26	-0.10
410	140	34	0.62	- 40	0.28	-0.34
420	200	6	1.52	- 76	0.39	-1.14
430	260	40	0.81	- 64	0.40	-0.42
440	330	270	0.09	110	0.31	0.23
450	450	420	0.03	240	0.40	0.40
460	570	550	0.02	320	0.40	0.38
470	680	650	0.02	340	0.34	0.32
480	750	750	0.00	320	0.24	0.24
490	950	900	0.02	280	0.19	0.16
500	1100	1050	0.02	220	0.12	0.10
510	1300	1250	0.02	160	0.08	0.06
520	1500	1450	0.02	200	0.08	0.06
530	1700	1500	0.05	160	0.10	0.05
540	1800	1500	0.08	-120	0.05	-0.03
550	1900	1500	0.10	-240	0.04	-0.06
560	1950	1750	0.05	- 50	0.04	-0.01
570	1950	1850	0.02	0	0.02	0.00
580	1950	1770	0.04	-120	0.01	-0.03
590	1950	1800	0.04	20	0.04	0.00
600	1950	1850	0.02	20	0.03	0.00
610	1950	1900	0.01	20	0.02	0.00
620	1950	1900	0.01	20	0.02	0.00
630	1950	1900	0.01	20	0.02	0.00
640	1950	1850	0.02	20	0.03	0.00
650	1900	1800	0.02	40	0.03	0.01
660	1750	1650	0.03	20	0.03	0.01
670	1450	1350	0.03	40	0.04	0.01
680	1050	950	0.04	60	0.07	0.03
690	800	750	0.03	40	0.05	0.03
700	800	750	0.03	40	0.05	0.02

A,gs: ground state absorbance = log Io/I
Io: light transmitted by cell filled with buffer = 100% T; detected as a voltage;
I: light transmitted by sample, detected as a voltage;
ΔV: maximum voltage change after flash;
A,triplet: log Io/(I-ΔV);
ΔA: triplet-singlet difference = log (I-ΔV)/I

FIGURE 5.3

^{3}Znc/$\overline{\text{Znc}}$ DIFFERENCE SPECTRUM - 11.1 μM Znc in 1 mM phosphate buffer, pH 7.

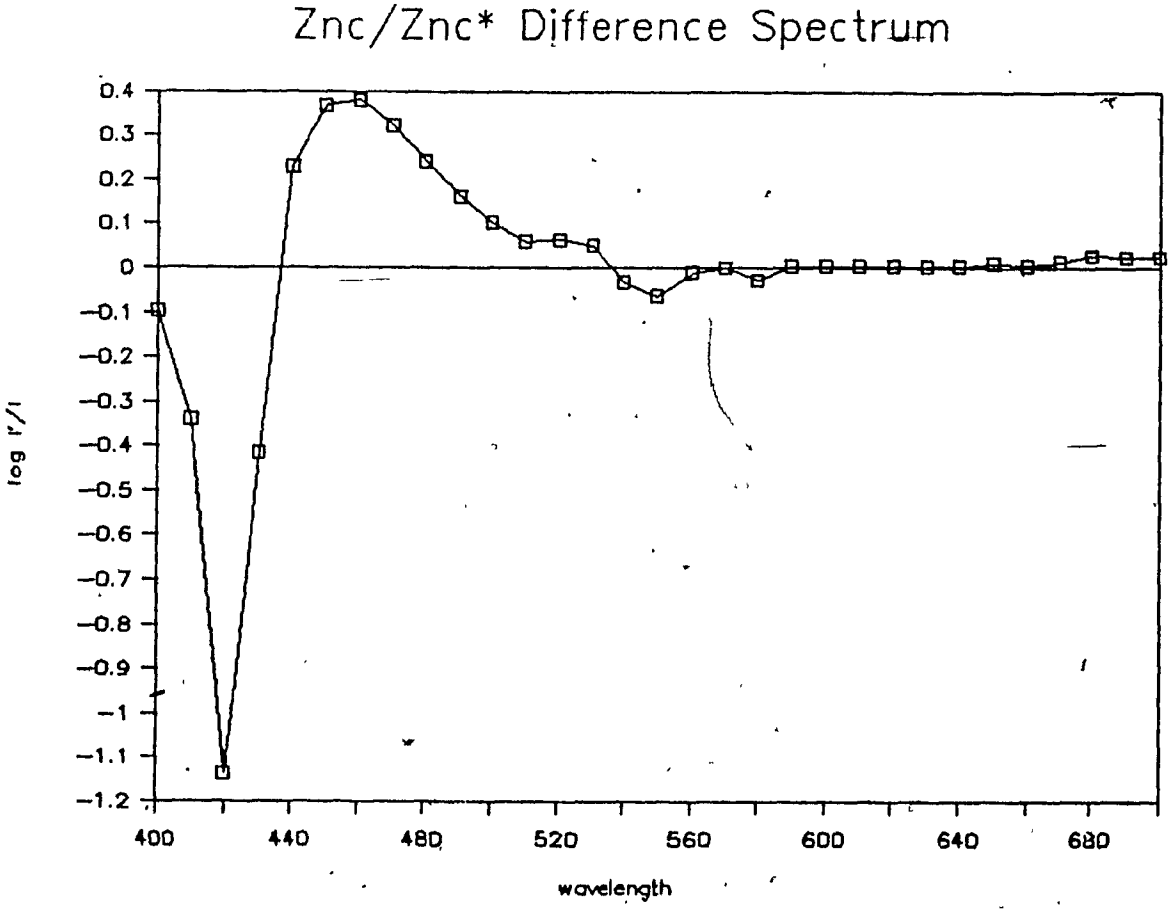
Znc/Znc* Difference Spectrum
0.4
0.3
0.2
0.1
0
−0.1
−0.2
−0.3
−0.4
−0.5
−0.6
−0.7
−0.8
−0.9
−1
−1.1
−1.2
log I'/I
400
440
480
520
560
600
640
680
wavelength

5.4.2 Znc TRIPLET EMISSION SPECTRUM

The triplet emission spectrum was recorded in the dark, @ 800 V applied on the PMT. Fig 5.4 shows that maximum emission occurs at 738 and 800 nm. At all wavelengths, emission lifetime was the same as that of absorption.

TABLE 5.2: Experimental Measurements recording the ^{3}Znc Emission Spectrum. λ_{ex}:578 nm.

λ, nm	I, mV
700	6
710	28
720	42
730	66
736	74
740	70
750	46
760	30
770	24
780	20
790	20
800	30
810	22
820	15

FIGURE 5.4

^{3}Znc TRIPLET EMISSION SPECTRUM - 11.1 μM Znc in 1 mM phosphate buffer, pH 7.

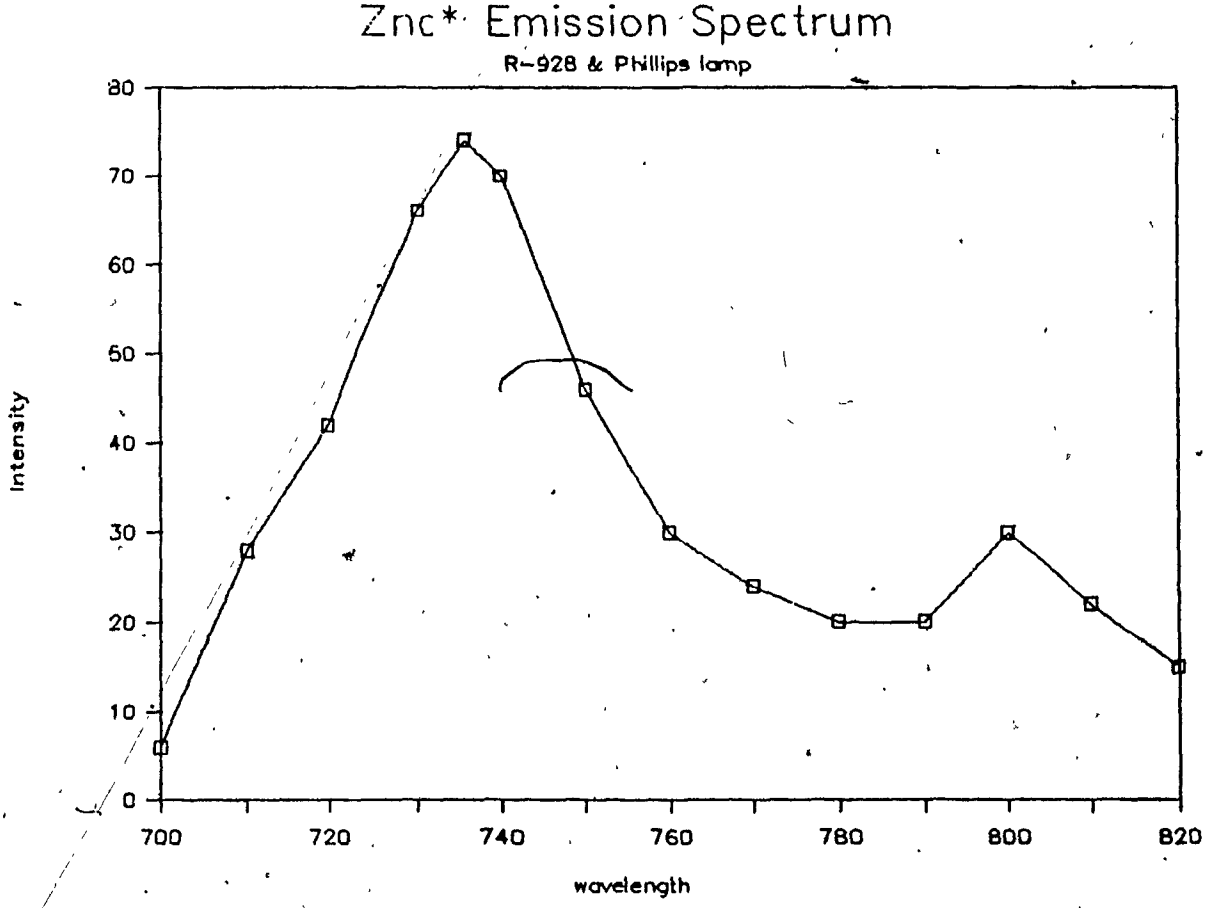
Znc* Emission Spectrum
R-928 & Phillips lamp
Intensity
80
70
60
50
40
30
20
10
0
700
720
740
760
780
800
820
wavelength

5.4.3 QUENCHING EXPERIMENTS

Table 5.3 summarizes the ^{3}Znc quenching experiments, performed as described in section 5.2.1

TABLE 5.3: ^{3}Znc Triplet Quenching Results @ 464 nm

Sample	Process	Decay rate, s^{-1}
^{3}Znc	Single exponential	k = 92 ± 5
^{3}Znc:$a^3a_3^3$ complex	Sum of two exponenials	k_f = 668 ± 23
		k_s = 330 ± 19
^{3}Znc:$a^2a_3^2$ complex	Sum of two exponentials	k_f = 1276± 22
		k_s = 324 ± 17
^{3}Znc:c^2	Single exponential	k = 95 ± 5

Quenching was also monitored at 432 nm (^{3}Znc/Znc isosbectic), at 602 nm, where amaximum change of absorbance would be expected if haem a were to be reduced, at 586 and 605 nm and finally in the 620-680 range where $Znc^{\cdot+}$ growth would be expected. Flashing at ^{3}Znc/Znc isosbectics produced no absorbance changes whatsoever and flashing at those wavelengths where the ^{3}Znc/Znc difference was observable yielded rate constants with the same magnitude as those shown in table 5.3 .

Fig 5.5 shows a trace recorded for the oxidized complex and Fig 5.6 one obtained for the reduced complex.

FIGURE 5.5

TRIPLET ABSORPTION DECAY of Zn:aa_3- monitored at 464 nm. The 1:1 complex was eluted on Sephadex G-75 and flashed as described in section 5.4.3. Conditions: 0.001 M KPi, μ = 0.0012 M; pH = 7. [A] Trace recorded; [B] Weighted least-squares on the fast component ($k = 668\ s^{-1}$) and [C] on the slow componet ($k = 330\ s^{-1}$). The same results were obtained using the simplex program.

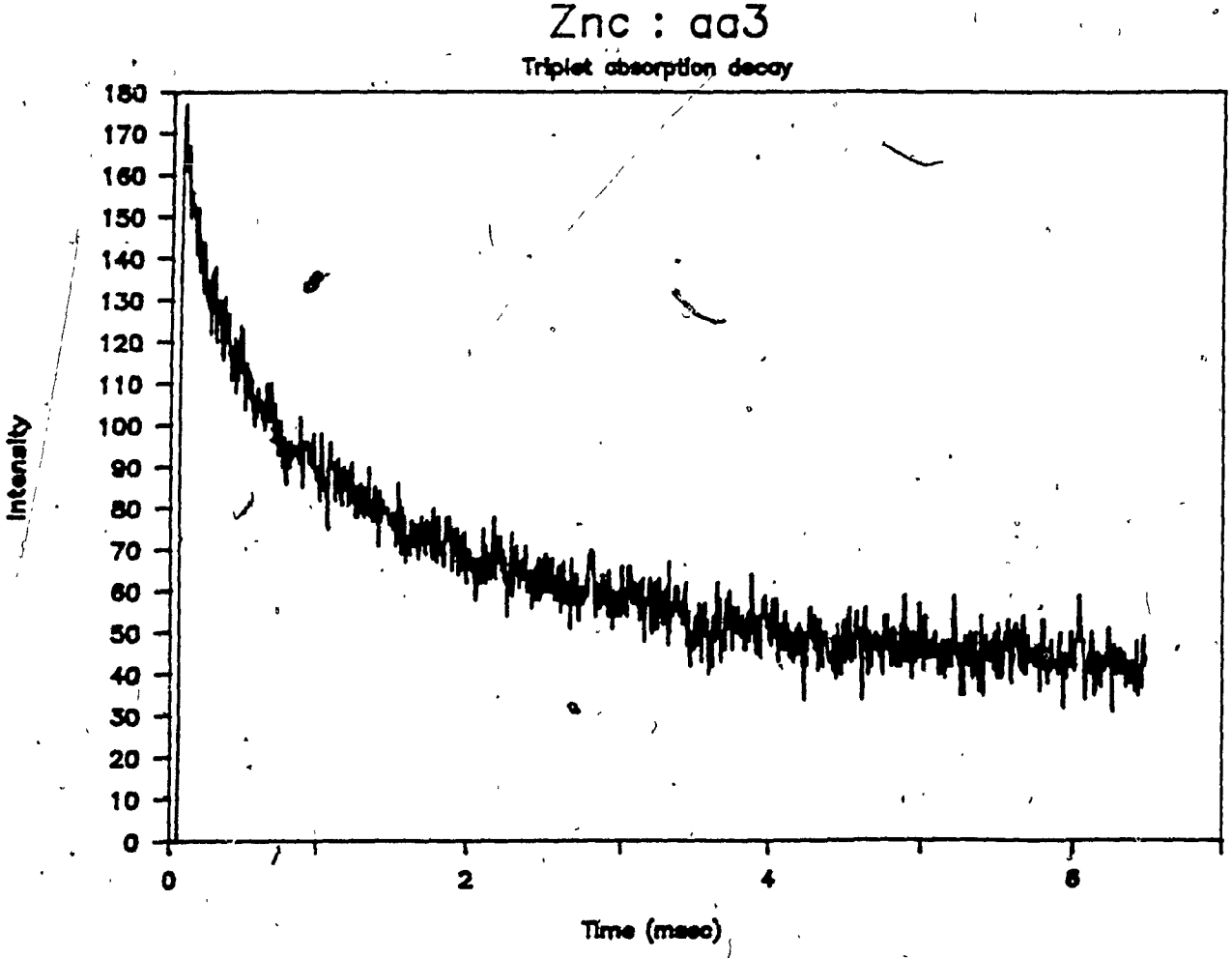
Znc : aa3
Triplet absorption decay
Intensity
180
170
160
150
140
130
120
110
100
90
80
70
60
50
40
30
20
10
0
0
2
4
6
Time (msec)

[A]

[B]

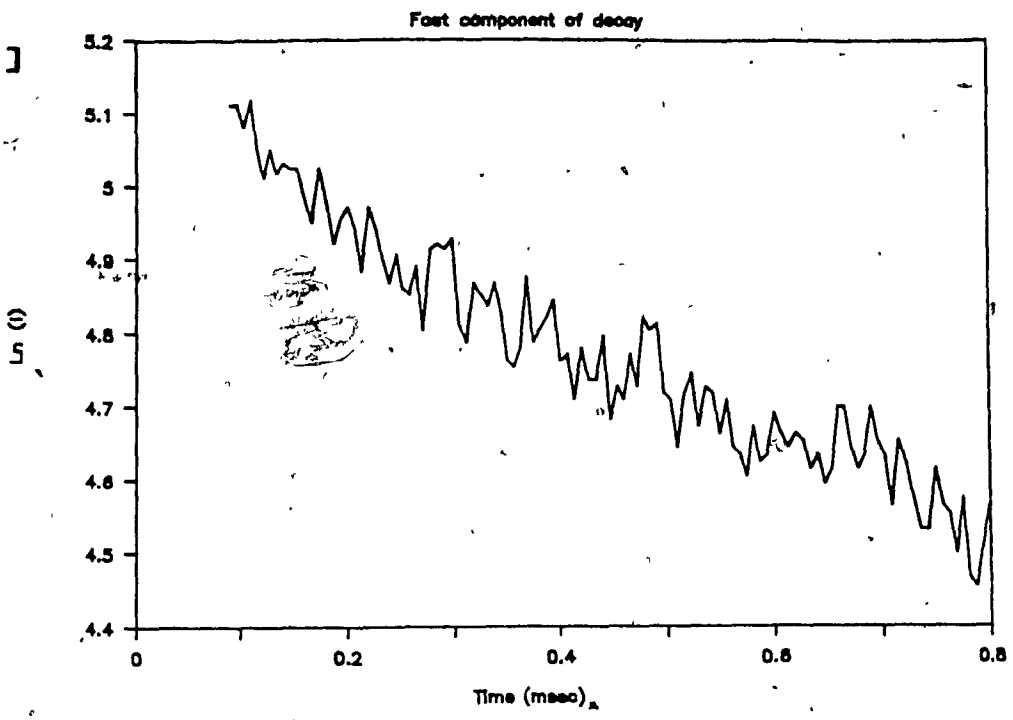
Znc : aa3
Fast component of decay
5.2
5.1
5
4.9
4.8
4.7
4.6
4.5
4.4
0
0.2
0.4
0.6
0.8
Time (msec)

[C]

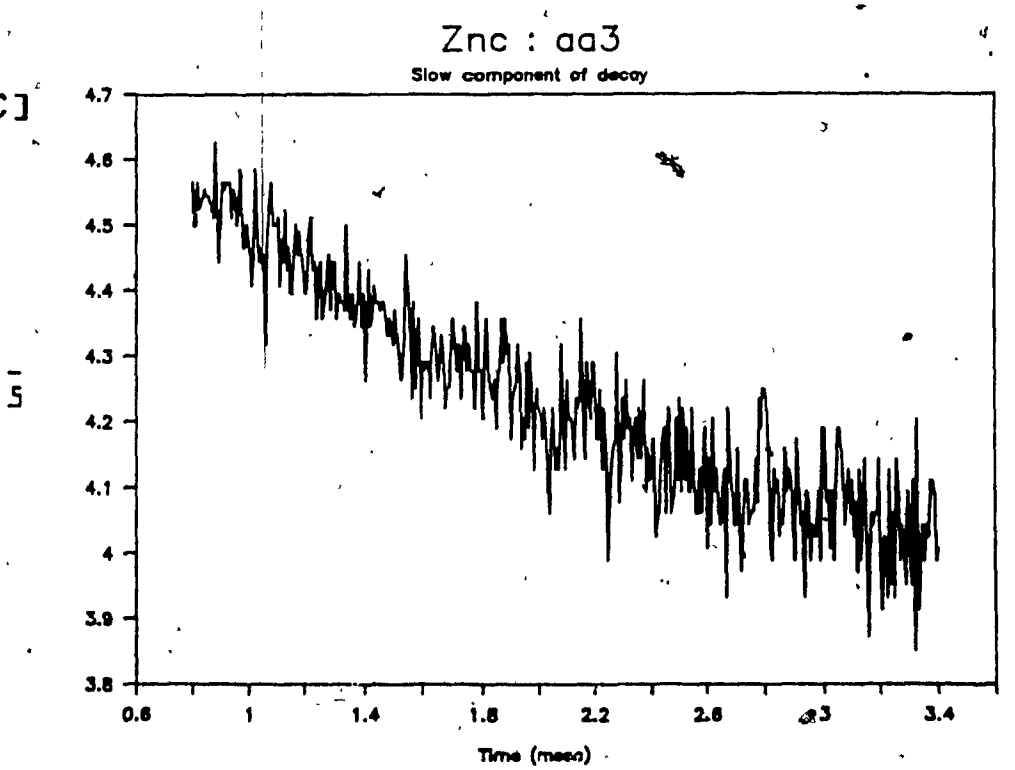
Znc : aa3
Slow component of decay
4.7
4.6
4.5
4.4
4.3
4.2
4.1
4
3.9
3.8
0.6
1
1.4
1.8
2.2
2.6
3
3.4
Time (msec)

FIGURE 5.6

TRIPLET ABSORPTION DECAY of Znc:$a^2a_3^2$ - monitored at 464 nm. In a typical experiment, the oxidized complex was flashed, stoichiometric amounts of sodium dithionite were added and once the Cary recorded spectrum showed full reduction, the sample was again flashed. F-CURVE yields a best fit using a sum of two exponentials with k_{fast} = 1276 s^{-1} and k_{slow} = 324 s^{-1}. Least-squares gives the same result.

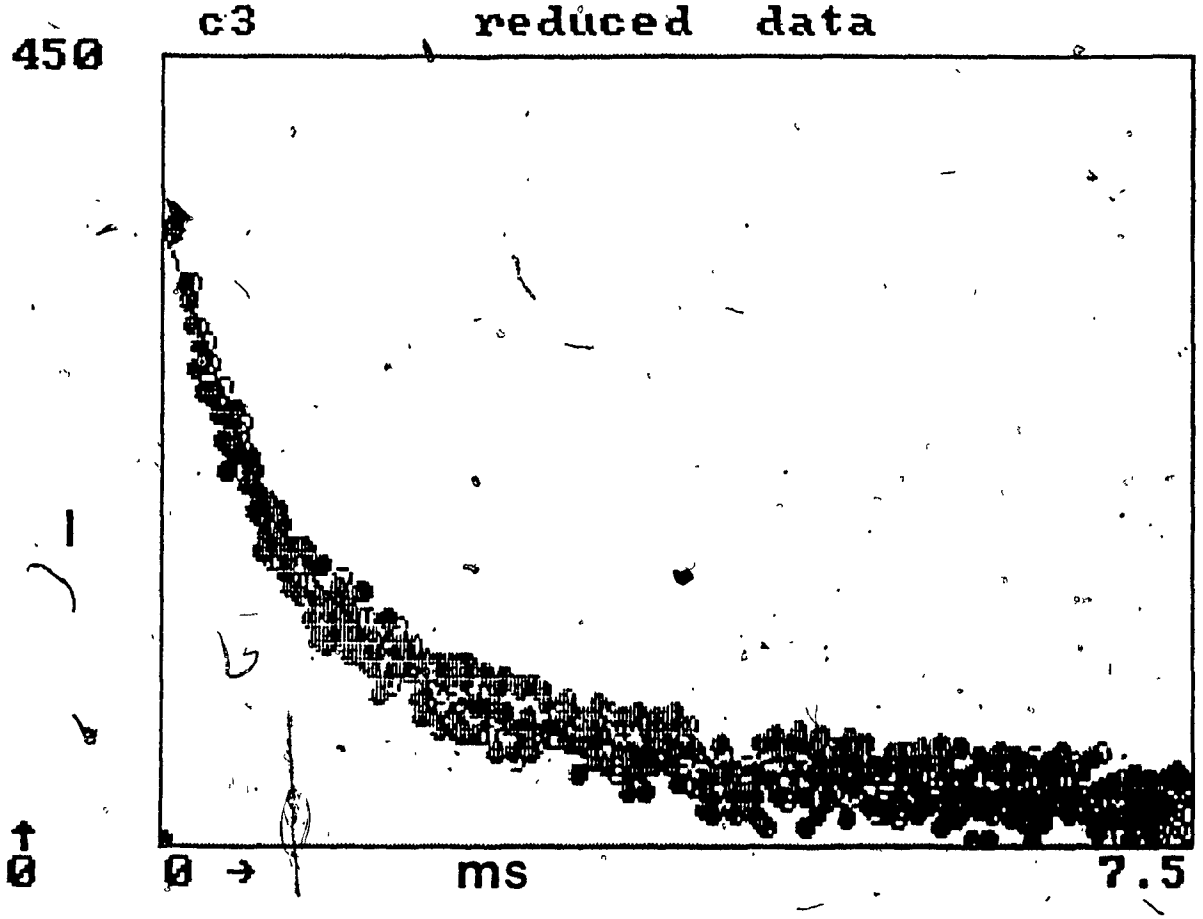
c3
reduced data
450
I
0
0 →
ms
7.5

5.4.4 CALCULATION OF THE OVERLAP INTEGRAL FOR $^{9}Zn_{C}$ EMISSION AND OXIDASE ABSORPTION

The overlap intergral J is defined by equation 2.3 .It can be evaluated using Simpson's rule, which yields a good approximation of the overlap area between the emission spectrum of the donor and the absorption spectrum of the acceptor. Table 5.4 lists the parameters relevant to the evaluation of J.

Simpson's rule can be expressed as follows:

$$\int_a^b f(x)dx = \frac{b-a}{3n}[f(x_0) + 4f(x_1) + 2f(x_2) + 4f(x_3) + \ldots + 2f(x_{n-2}) + 4f(x_{n-1}) + f(x_n)] \qquad (5.4)$$

From Table 5.4 we can calculate:

$$\Sigma k_{\upsilon}.I_{em} = 1252 \qquad (5.5)$$

and: $$\Sigma f(x_i) = 81.68 \times 10^{-12}\ cm^{-3}M^{-1} \qquad (5.6)$$

while: $$b - a / 3n = 3.16 \times 10^{-7} \qquad (5.7)$$

We can now proceed to evaluate:

$$J = \frac{\int_a^b I_{em}(\lambda)\ \varepsilon_A(\lambda)\lambda^4\ d\lambda}{\int_a^b I_{em}(\lambda)\ d\lambda} \qquad (5.8)$$

$$J = \frac{(3.16 \times 10^{-7})\ (81.68 \times 10^{-12})}{(3.96 \times 10^{-4})} \qquad (5.9)$$

$$J = 3.31 \times 10^{-14}\ cm^{-3}M^{-1} \qquad (5.10)$$

TABLE 5.4: Evaluation of ^{3}Zn-oxidase(ox) Overlap Integral by Simpson's Rule from 640 to 820 nm.

λ,cm.10^{5}	λ,cm^{4}.10^{17}	$\varepsilon_{A}(\lambda)$,cm^{-1}M^{-1}.10^{-3}	Iem(λ)
6.40	1.67	6.61	1
6.50	1.79	5.95	1
6.60	1.90	5.33	1
6.70	2.02	4.41	5
6.80	2.14	3.52	5
6.90	2.27	2.86	5
7.00	2.40	2.43	6
7.10	2.54	2.20	28
7.20	2.69	2.20	42
7.30	2.84	2.20	66
7.40	3.00	2.42	70
7.50	3.16	2.64	46
7.60	3.34	2.69	30
7.70	3.52	2.73	24
7.80	3.70	3.08	20
7.90	3.90	3.10	20
8.00	4.10	3.15	30
8.10	4.30	3.17	22
8.20	4.52	3.17	15

k_i	k_i x Iem(λ)	f(x).10^{-12},cm^{-3}M^{-1}
1	1	00.110
4	4	00.426
2	2	00.203
4	20	01.782
2	10	00.753
4	20	01.298
2	12	00.698
4	112	06.259
2	84	04.971
4	264	16.495
2	140	10.164
4	184	15.350
2	60	05.391
4	96	09.225
2	40	04.558
4	40	04.836
2	60	07.749
4	88	11.995
1	15	02.149

ε_{A} values on a haem a_3 basis-

k_i = Simpson factor -

The overlap integral can also be evaluated for the reduced form of the oxidase, by using the appropriate extinction coefficients. These calculations yield:

$$J = 1.23 \times 10^{-15} cm^{-9} M^{-1} \qquad (5.11)$$

Ro, the critical radius for energy transfer (V. section 2.2) in the Förster formalism can be calculated using the overlap integrals evaluated above. With:

$$Ro(A) = (JK^2 \phi_o n^{-4})^{1/6} (9.79 \times 10^9) \qquad (5.12)$$

and using K = 1; n = 1.4 [Vanderkooi,1975] and ϕ_o = 0.0044 [Dixit,1981], the Ro values listed in Table 5.5 can be obtained.

TABLE 5.5: Critical Radii for Dipole-Dipole Energy Transfer between ^{3}Zn$\subset$ and Cytochrome $\subset$ Oxidase.

Overlap	J,($cm^{-9}M^{-1}$)	Ro,(A)
$^3Zn\subset : a^3Cu_A^2 a_3^3Cu_B^2$	3.31×10^{-14}	18
$^3Zn\subset : a^2Cu_A^1 a_3^2Cu_B^1$	1.23×10^{-15}	10

5.5 DISCUSSION

The ^{3}Znc/Znc difference spectrum obtained in this work (Fig 5.3) is in very good agreement with that published by Elias *et al.*(Fig 3.2). The shoulder observed at 525 nm further characterizes this spectrum as these authors did not cover this range, having measured at 25 - 50 nm-intervals (vs. 10 nm-intervals in this work). Results also show that only one excited Znc state is involved, as no wavelength dependence was observed in the mesured decay rates. That native cytochrme c does not quench the excited state is indicative of a quenching process due to either electron or energy transfer, as both processes can not occur with cytochrome c, the former because it is reduced and the latter because no donor-acceptor overlap exists.

Intramolecular electron transfer could be invoked by the following scheme:

$$Znc{:}a^3Cu_A^2a_3^3Cu_B^2 \underset{k_d}{\longrightarrow} {}^3Znc{:}a^3Cu_A^2a^3Cu_B^2 \xrightarrow{k_{et}} Znc^{\cdot+} + aCu_A^+a^3Cu_{B(red)} \qquad (5.13)$$

With such a scheme, the decay rate of ^{3}Znc is first order, with the observed quenching rate $k_q = k_d + k_{et}$. Substituting the observed quenching rates (668 s^{-1} and 330 s^{-1}) and the Znc decay rate of 92 s^{-1} yields values of 576 s^{-1} and 238 s^{-1} for the formation of electron transfer products which can

either be a form of the reduced oxidase or the Zn*c* radical. Results show clearly that no such evidence was observed and that energy transfer is a more likely quenching process, as shown by the quenching observed with the fully reduced form of the oxidase. As with the oxidized oxidase, the reduced quenching features two processes of the same order of magnitude (1276 s^{-1} and 324 s^{-1}). This eliminates electron transfer as a possible quenching mechanism and the question of interest is now to determine acceptor distances.

The distance R between a donor and its acceptor can be calculated using equation 2.1 which can be rewritten as:

$$R = R_o(k_o/k_T)^{1/6} \qquad (5.14)$$

Using K_o = 92 s^{-1} and k_T = 668 s^{-1} and 330 s^{-1} for both components of the decay the donor-acceptor distances calculated are 13 A and 15 A, respectively.

Likely acceptors at distances of 13 and 15 A can only be haem *a* or Cu_A. Haem a_3 and Cu_B can be eliminated as neither significantly contributes to the absorption spectrum in this range [Boelens,1980]. The spectral feature of interest is the 640 nm-shoulder in the oxidase absorption spectrum. If it is taken to be the tail of the 598 nm-haem *a* band, then the two quenching processes observed could be the sum of two contributions : a d-d transfer to Cu_A (R = 13 A) and a transfer to haem *a* (R = 15 A). In this case, the 15 A- haem *a* to *c* distance would contrast with previous determinations of 25 A and more [V. Table 2.1]. In their Zn*c* fluorescence work,

Alleyne & Wilson discounted copper atoms as acceptors, although they admitted that weak copper absorption bands could lie beneath the α and β oxidase bands [Alleyne,1987]. Their reasoning was correct in that ligand field treatment of the aqueous absorption characteristics of divalent, square-planar copper complexes show weak absorption in the 450 -650 range, followed by the broad absorption band with maximum at 833 nm [Figgis,1964]. That the 640-nm shoulder belongs to copper is shown by the work of Weintraub *et al.* who showed that the spectrum of copper-depleted oxidase lacks the shoulder [Weintraub,1981]. Further, Glatz *et al.* in their investigation of energy transfer between copper cytochrome c and the oxidase point out that energy transfer from the porphyrin triplet to a copper of cytochrome oxidase is not spin-forbidden [Glatz, 1979].

On the basis of the previous considerations, it is therefore reasonable to propose the following interpretation:

Dipole-dipole transfer of the triplet excitation energy occurs between Znc and two acceptors in cytochrome c oxidase, located at 13 and 15 A from Znc. One of these coppers is Cu_A and the other is either the "third" copper reported by some groups to be present in the oxidase [Brudvig,1981] or the Cu_A of a second oxidase molecule. Referring to Fig 1.6 shows a model of a dimeric oxidase which features sharing one cytochrome c per dimer. Previous work in this laboratory [Kornblatt,1986] has shown that, at low ionic strength, the

binding of porphyrin c to the oxidase is such that a single bound porphyrin c communicates with four haem a and four Cu, thus providing evidence for the concept of a four-haem, four-copper functional unit of the oxidase. In the light of this work, the second Cu acceptor belonging to another oxidase molecule becomes an attractive possibility.

REFERENCES

Alleyne, T. A. and M.T. Wilson, Biochem. J. 247, 475 (1987).

Boelens, R. and R. Wever, R. FEBS Lett. 116, 223 (1980).

Brudvig, G. W. The Nature and Distribution of the Metal Centers in Cytochrome c Oxidase; Thesis, CalTech, 1981. UMI-8104669.

Demas, J. N. Excited State Lifetime Measurements, Academic Press, New York, 1983.

Figgis, B. N. Introduction to Ligand Fields, Interscience Publishers, New York, 1964.

Glatz, P.; Chance, B. and J.M. Vanderkooi, Biochem. 18, 3466(1979).

Kornblatt, J. A. and H.A. Luu, Eur. J. Biochem. 159, 407 (1986).

Noggle, J. H. Physical Chemistry on a Microcomputer, Little, Brown & Co., Boston, 1985.

Noggle, J. H. F-CURVE; software copyright 1985.

Vanderkooi, J. M. and M. Erecinska, Eur. J. Biochem.60, 199(1975).

Weintraub, S.T. and D. C. Wharton, J. Biol. Chem. 256, 1669 (1981).

6. CONCLUSION

"Spectral changes,
What are they ?
Mechanistic Overlay.
When it sticks,
You've got a lot.
But can you name
The path it shot?"
E. Castro

It is with confidence that this thesis proposed coppers as likely energy acceptors and any remaining uncertainty could soon be dismissed by performing the one experiment which time constraints unfortunately did not allow: monitor quenching of Zn*c* fluorescence by the oxidase. The picosecond facilities are available at Concordia and the timescale of observation ($\tau_f \leq 1.4$ ns) is well within the detection limits of the picosecond center's instrumentation. With fluorescence maxima at 590 and 640 nm, there is no question that haem *a* would be the acceptor and that the 640 nm results could be used to confirm or disprove copper as an acceptor. Expected intermolecular distances with haem *a* acceptors would be in the $\geq$ 25 A range.

The laboratory now has a reproducible procedure for the preparation of zinc and tin cytochrome *c* as well as the potential of breaking new ground with europium cytochrome *c*. Rare earths have sharp emission transitions and are used in inorganic research to elucidate their site occupancies with considerable success. It is only a question of time for biochemists to adopt them as probes and extract from them a body of structure-function information as valuable as

that provided by the contributions of transition metal bioinorganic chemistry.

The contributions of this work can be summarized as follows:

- Reproducible synthesis of Sn$\underline{c}$ and Zn$\underline{c}$;
- Fluorescence decay measurements on both species;
- Preparation of a stable Eu$\underline{c}$ at pH < 5;
- Demonstration that energy transfer predominates over electron transfer in the ^{3}Zn$\underline{c}$:oxidase couple;
- Determination of the distance from $\underline{c}$ to oxidase coppers of 13 and 15 Å.